

# Excited spherical waves in unbounded cold magnetoplasma and applications in radio sounding

Xueqin Huang<sup>1</sup> and Bodo W. Reinisch<sup>1,2</sup>

Received 29 November 2011; revised 29 February 2012; accepted 1 March 2012; published 18 April 2012.

[1] The electromagnetic field excited by an arbitrary current source embedded in an unbounded uniform cold magnetoplasma is investigated in this paper. The Green's function method for solving the radiation equation is used, and the derived solution is valid for any cold plasma parameters. There are always two wave modes excited, and in the far field each mode has the form of a spherical wave. A refractive index for spherical waves is introduced to describe the propagation. The properties of these excited spherical waves are discussed in this paper in comparison with the plane wave representation. It is shown that the energy flow of the spherical wave is always in the radial direction, i.e., parallel to the wave normal.

**Citation:** Huang, X., and B. W. Reinisch (2012), Excited spherical waves in unbounded cold magnetoplasma and applications in radio sounding, *Radio Sci.*, 47, RS0L08, doi:10.1029/2011RS004940.

## 1. Introduction

[2] When a radio sounder in the ionosphere or magnetosphere transmits electromagnetic waves, these waves can return to the receiver when they are reflected in the plasma. The received signals provide the information of the sounded media. By analyzing the measured data, the physical parameters of the medium like density and movement can be obtained. The waves usually originate from a source of small dimensions relative to the distances involved, and in the far field they have spherical wavefronts. For ground-based sounding, when the wave reaches the ionosphere the radius of curvature is so large that the wave in a given direction can be treated as one of two plane waves, either L mode or R mode, and the error introduced with this approximation is generally believed to be negligibly small. For sounding in the topside ionosphere and the magnetosphere, however, the transmitter and receiver on board a rocket or satellite are located within an anisotropic medium, and the question arises as to how well the excited field is still approximated by a single plane wave in a given direction.

[3] The radiation problem for a source located in an anisotropic medium was first addressed in the middle of the last century [Arbel and Felsen, 1963, and references therein]. Later several methods were proposed to study radiation in anisotropic plasma [Seshadri and Wu, 1970; Bennett, 1976; Fung and Kwan, 1983; Lai and Chan, 1986; Novikov and Rybachek, 1990; Cottis et al., 1999], and solutions were found for a point source or an elementary dipole. For a given current distribution, the radiation field is a superposition of the contributions from all the source points of the current. In the integration process, however, difficulties arose in finding

rigorous analytical expressions for the radiation field, except for some special current distributions [Bennett, 1976]. Special attention was paid to studying the characteristics of short antennas in plasma [e.g., Balmain, 1964; Chevalier et al., 2008]; near field approximations or numerical methods were used for these analyses. In this paper, we derive analytical solutions for the far field that can be used for radio sounding applications like the Radio Plasma Imager (RPI) on NASA's IMAGE satellite with dipole antennas extending 500 m tip to tip and operating frequencies from 3 kHz to 3 MHz [Reinisch et al., 2000, 2001].

[4] An attempt is made in this paper to derive the electromagnetic waves in the far field excited by a current source arbitrary in dimension and distribution, and to study the excited wave properties including wave mode, polarization, and the energy flow when the current source is embedded in anisotropic plasma. Applications to inhomogeneous media [e.g., Fung and Green, 2005] are not attempted here, and will be reported in a future paper.

## 2. Assumptions and the General Solution

[5] It is assumed that a sinusoidal current source is located in an unbounded uniform magnetoplasma described by the cold plasma theory, and that a sinusoidally varying electromagnetic field will be stimulated; the  $e^{j\omega t}$  term is deleted in the equations below. When the z axis is set along the direction of the ambient magnetic field, the relative dielectric tensor  $\epsilon$  can be written in matrix form [Budden, 1985]

$$\epsilon = \begin{bmatrix} \epsilon_1 & -j\epsilon_2 & 0 \\ j\epsilon_2 & \epsilon_1 & 0 \\ 0 & 0 & \epsilon_3 \end{bmatrix}, \quad \begin{cases} \epsilon_1 = 1 - \frac{XU}{U^2 - Y^2}, \epsilon_2 = \frac{XY}{U^2 - Y^2}, \epsilon_3 = 1 - \frac{X}{U} \\ X = \frac{\omega_{pe}^2}{\omega^2}, Y = \frac{\omega_{ce}}{\omega}, U = 1 - jZ, Z = \frac{\nu}{\omega} \end{cases} \quad (1)$$

<sup>1</sup>Center for Atmospheric Research, University of Massachusetts Lowell, Lowell, Massachusetts, USA.

<sup>2</sup>Lowell Digisonde International, LLC, Lowell, Massachusetts, USA.

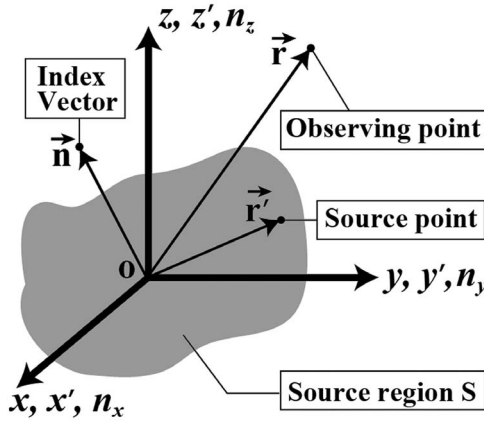


Figure 1. Coordinate systems.

where  $\omega$  denotes the angular frequency, and  $\nu$  the electron-neutral collision frequency. The electron plasma frequency  $\omega_{pe}$  and the electron gyrofrequency  $\omega_{ce}$

$$\begin{aligned}\omega_{pe} &= (N_e e^2 / \epsilon_0 m_e)^{1/2} \\ \omega_{ce} &= |e| B_0 / m_e\end{aligned}\quad (2)$$

depend on the plasma density ( $N_e$ ), electron charge ( $e$ ) and mass ( $m_e$ ), and the amplitude of the ambient magnetic field intensity ( $B_0$ ). It should be noted that the ion effects have been ignored in equation (1) although that is not necessary in this study.

[6] The goal of this analysis is to find the solution from the equation derived from the Maxwell equation system

$$\nabla \times (\nabla \times \mathbf{E}(\mathbf{r})) - k_0^2 \boldsymbol{\epsilon} \cdot \mathbf{E}(\mathbf{r}) = -j\mu_0 \omega \mathbf{J}(\mathbf{r}) \quad (3)$$

where  $\mathbf{J}(\mathbf{r})$  is the complex current density at a source point.  $\mathbf{E}(\mathbf{r})$  and  $\mathbf{H}(\mathbf{r})$  are the phasors of the electric and magnetic fields at the observation point  $\mathbf{r}$ , and  $k_0 = \omega/c$  is the wave number in free space. The relationship between the speed of light in free space,  $c$ , the permittivity of free space,  $\epsilon_0$ , and the permeability of free space,  $\mu_0$ , is  $c = 1/\sqrt{\epsilon_0 \mu_0}$  in the International System of Units. Bold letters denote vectors or tensors, and this notation convention applies throughout the text of this paper.

[7] This analysis is not limited to any specific current source as long as it is confined to a limited region of space. In general, a rigorous solution of equation (3) can be derived with the Green's function method [Weiglhofer, 1993; Bayin, 2006a, 2006b]. The Green's function is a tensor,

$$\begin{aligned}\mathbf{G}(\mathbf{r}, \mathbf{r}') &= \frac{j\mu_0 \omega}{(2\pi)^3} \int \left\{ \Gamma^{-1} e^{-j\mathbf{k} \cdot (\mathbf{r} - \mathbf{r}')} \right\} d\mathbf{k} = \frac{j\mu_0 \omega k_0^3}{(2\pi)^3} \\ &\cdot \int \left\{ \Gamma^{-1} e^{-jk_0 \mathbf{n} \cdot (\mathbf{r} - \mathbf{r}')} \right\} d\mathbf{n} \\ \Gamma &= \mathbf{k}\mathbf{k} - k^2 \mathbf{I} + k_0^2 \boldsymbol{\epsilon} = k_0^2 (\mathbf{n}\mathbf{n} - n^2 \mathbf{I} + \boldsymbol{\epsilon})\end{aligned}\quad (4)$$

where  $\mathbf{I}$  denotes the unit tensor. The solution of equation (3) is then

$$\mathbf{E}(\mathbf{r}) = \frac{j\mu_0 \omega k_0^3}{(2\pi)^3} \int d\mathbf{n} \left\{ e^{-jk_0 \mathbf{n} \cdot \mathbf{r}} \Gamma^{-1} \cdot \int d\mathbf{r}' [e^{jk_0 \mathbf{n} \cdot \mathbf{r}'} \mathbf{J}(\mathbf{r}')] \right\}. \quad (5)$$

In equations (4) and (5)  $\int \dots d\mathbf{r}'$ ,  $\int \dots d\mathbf{k}$ , or  $\int \dots d\mathbf{n}$  are simplified notations for the three-dimensional integrals, and the

refractive index vector of a plane wave,  $\mathbf{n}$ , is defined proportional to the wave vector  $\mathbf{k}$  by

$$\mathbf{k} = k_0 \mathbf{n}. \quad (6)$$

When the adjoint matrix of  $\Gamma$  is denoted by  $\text{adj}(\Gamma)$  and its determinant is denoted by  $\det(\Gamma)$ , the inverse matrix  $\Gamma^{-1} = \text{adj}(\Gamma)/\det(\Gamma)$ . The integration for the current in (5) is the spatial spectrum of the current in  $n$  space given by its Fourier transform,

$$\mathbf{J}(\mathbf{n}) = \int d\mathbf{r}' [\mathbf{J}(\mathbf{r}') e^{jk_0 \mathbf{n} \cdot \mathbf{r}'}] \quad (7)$$

In the following analysis, three coordinate systems are defined for the observing point, the current source, and the refractive index space, as shown in Figure 1. Their common origin is selected at a point inside the current source region, and the  $z$  axes are parallel to the ambient magnetic field. In addition to the Cartesian coordinate systems we also selectively use spherical and cylindrical coordinate systems to facilitate the calculations, transforming from one to another as needed. The components are denoted as

$$\begin{aligned}\mathbf{r} &= (x, y, z) = (r, \alpha, \beta) = (\rho, \beta, z) \\ \mathbf{r}' &= (x', y', z') = (r', \alpha', \beta') = (\rho', \beta', z') \\ \mathbf{n} &= (n_x, n_y, n_z) = (n, \theta, \varphi) = (n_\rho, \varphi, n_z)\end{aligned}\quad (8)$$

Note that in addition to the three integrals in equation (7), the calculation of the electric field as expressed by equation (5) involves nine integrations over  $n$  space. As differentiation is in general easier than integration, the analysis is simplified by using the method developed by Kogelnik [1960]. In fact, part of the integrand can be replaced by the result of a differential operation because

$$\text{adj}(\Gamma) e^{-jk_0 \mathbf{n} \cdot \mathbf{r}} = \boldsymbol{\Lambda} e^{-jk_0 \mathbf{n} \cdot \mathbf{r}} \quad (9)$$

The differential operator  $\boldsymbol{\Lambda}$  is a tensor acting on the observing coordinates, and in the Cartesian coordinate system it can be written in a matrix form,

$$\boldsymbol{\Lambda} = \begin{bmatrix} \Lambda_{11} & \Lambda_{12} & \Lambda_{13} \\ \Lambda_{21} & \Lambda_{22} & \Lambda_{23} \\ \Lambda_{31} & \Lambda_{32} & \Lambda_{33} \end{bmatrix}. \quad (10)$$

The expression of the elements can be found in Appendix A. Applying equation (9) to (5) leads to

$$\mathbf{E}(\mathbf{r}) = \frac{j\mu_0 \omega k_0^3}{(2\pi)^3} \int d\mathbf{n} \left\{ \frac{\boldsymbol{\Lambda} e^{-jk_0 \mathbf{n} \cdot \mathbf{r}}}{\det(\Gamma)} \cdot \mathbf{J}(\mathbf{n}) \right\}. \quad (11)$$

As the integration over  $n$  space and the differentiation of the operator with respect to the observing point are independent, the computation order can be changed. Finally the expression of the radiation field becomes

$$\begin{aligned}\mathbf{E}(\mathbf{r}) &= \boldsymbol{\Lambda} \cdot \mathbf{A}(\mathbf{r}) \\ \mathbf{H}(\mathbf{r}) &= \frac{j}{\mu_0 \omega} \nabla \times \mathbf{E}(\mathbf{r})\end{aligned}\quad (12)$$

Here a vector function is introduced,

$$\mathbf{A}(\mathbf{r}) = \frac{j\mu_0 \omega k_0^3}{(2\pi)^3} \int d\mathbf{n} \left\{ \frac{e^{-jk_0 \mathbf{n} \cdot \mathbf{r}}}{\det(\Gamma)} \mathbf{J}(\mathbf{n}) \right\} \quad (13)$$

To solve the problem for an isotropic medium, as is well known, one usually introduces a vector potential and expresses the magnetic field by means of a differential operator (the curl) acting on it. For the anisotropic medium, the problem is more complicated. However, as indicated by equation (12) the electric field can be expressed as an operation of a differential operator acting on the vector  $\mathbf{A}(\mathbf{r})$ , which is sometimes referred to as the general vector potential, or often simply as the vector potential. Now, one needs to perform only a single three dimensional integration for the vector potential followed by differentiations to get the excited electromagnetic field according to equation (12).

### 3. General Vector Potential

[8] Because of the symmetrical property of the medium as implied by equation (1), plane waves can propagate along the ambient magnetic field, and cylindrical waves in the perpendicular direction. It should therefore be possible to represent the result of equation (13) as a superposition of such waves. In order to do this, it is more convenient to use the cylindrical coordinate system, and the integration will be performed over the whole  $n$  space such that  $d\mathbf{n} = n_\rho dn_\rho d\varphi dn_z$ ,  $0 \leq n_\rho < +\infty$ ,  $0 \leq \varphi \leq 2\pi$ ,  $-\infty < n_z < +\infty$ .

[9] In the cylindrical coordinate system,  $\mathbf{n} = (n_\rho, \varphi, n_z)$ , the determinant takes the form

$$\det(\mathbf{\Gamma}) = k_0^6 \left\{ \begin{aligned} &\varepsilon_3 n_z^4 + [(\varepsilon_1 + \varepsilon_3)n_\rho^2 - 2\varepsilon_1 \varepsilon_3] n_z^2 \\ &+ \varepsilon_1 n_\rho^4 + (\varepsilon_2^2 - \varepsilon_1^2 - \varepsilon_1 \varepsilon_3) n_\rho^2 + (\varepsilon_1^2 - \varepsilon_2^2) \varepsilon_3 \end{aligned} \right\}, \quad (14)$$

and after factorization

$$\det(\mathbf{\Gamma}) = k_0^6 \varepsilon_3 (n_z^2 - n_{z+}^2)(n_z^2 - n_{z-}^2), \quad (15)$$

where

$$\begin{aligned} n_{z\pm}^2 &= [2\varepsilon_1 \varepsilon_3 - (\varepsilon_1 + \varepsilon_3)n_\rho^2 + q_\pm(n_\rho)] / (2\varepsilon_3) \\ q_\pm(n_\rho) &= \pm [(\varepsilon_1 - \varepsilon_3)^2 n_\rho^4 - 4\varepsilon_2^2 \varepsilon_3 n_\rho^2 + 4\varepsilon_2^2 \varepsilon_3^2]^{1/2} \\ &(-\pi/2 \leq \arg(q_+) < \pi/2, \pi/2 \leq \arg(q_-) < 3\pi/2) \end{aligned} \quad (16)$$

Note that  $\det(\mathbf{\Gamma}) = 0$  is the dispersion relation giving the refractive index of plane waves expressed in the cylindrical coordinate system. It should be pointed out that the refractive index of plane waves derived this way is exactly the same as the index derived using spherical coordinates. There are two wave modes designated by “+” and “-” signs, and  $q(n_\rho)$  serves as the mode discriminator. At the so called coupling point, where  $q(n_\rho) = 0$ , the mode is indeterminate and will convert from one to the other when crossing it [Budden, 1985].

[10] Substituting equation (15) into equation (13) and noting that

$$n_{z+}^2 - n_{z-}^2 = q_+(n_\rho) / \varepsilon_3 = -q_-(n_\rho) / \varepsilon_3 \quad (17)$$

one can represent the vector potential as

$$\begin{aligned} \mathbf{A}(\mathbf{r}) &= \mathbf{A}_+(\mathbf{r}) + \mathbf{A}_-(\mathbf{r}) \\ \mathbf{A}_\pm(\mathbf{r}) &= \frac{j\mu_0\omega}{(2\pi)^3 k_0^3} \int_0^\infty dn_\rho \left\{ \frac{n_\rho}{q_\pm(n_\rho)} \int_0^{2\pi} d\varphi \left[ e^{-jk_0 n_\rho \rho \cos(\varphi-\beta)} \right. \right. \\ &\quad \left. \left. \cdot \int_{-\infty}^{+\infty} dn_z e^{-jk_0 n_z z} \frac{\mathbf{J}(n_\rho, \varphi, n_z)}{n_z^2 - n_{z\pm}^2} \right] \right\} \end{aligned} \quad (18)$$

Equation (18) indicates that the vector potential, and thus the excited field, can be decomposed into two parts related to the two modes of plane wave.

[11] In collisional plasma, the integrand of integral (18) has four poles in the complex  $n_z$  plane, two located in the lower half plane, and two in the upper half plane. For collisionless plasma the poles are all located on the real axis. As the integration results for collisional and collisionless plasma are different, we use the limitation principle: the solution for collisional plasma is found, and then the solution for the collisionless plasma is determined as the limit of the general solution as the collisions approach zero. The integral over  $n_z$  can be performed using the residue theorem. There are possibly more poles associated with the spatial spectrum as discussed by *Kaklamani and Uzunoglu* [1992]. To simplify the analysis, it is assumed in this paper that there are no singular points for the spatial spectrum  $\mathbf{J}(n_\rho, \varphi, n_z)$  and that it vanishes at infinity, i.e.,  $\lim_{|n| \rightarrow \infty} \mathbf{J}(n_\rho, \varphi, n_z) = 0$ . When  $z > 0$

(or  $z < 0$ ), the real axis and the semicircle in the lower (or upper) half  $n_z$  plane are selected as the integration contour so that the poles enclosed in the lower (or upper) half plane are used for the integration. The results for the two cases can be combined into one representation associating only with the poles in the lower half plane,

$$\begin{aligned} \mathbf{A}_\pm(\mathbf{r}) &= \frac{\mu_0\omega}{(2\pi)^2 k_0^3} \int_0^\infty dn_\rho \left\{ \frac{n_\rho e^{-jk_0 n_{z\pm} \text{sgn}(z)z}}{2q_\pm n_{z\pm}} \int_0^{2\pi} d\varphi \right. \\ &\quad \left. \cdot \left[ e^{-jk_0 n_\rho \rho \cos(\varphi-\beta)} \mathbf{J}(n_\rho, \varphi, n_{z\pm} \text{sgn}(z)) \right] \right\} \\ &(z \neq 0; -\pi < \arg(n_{z\pm}) < 0) \end{aligned} \quad (19)$$

The sign function is defined as

$$\text{sgn}(z) = \begin{cases} -1, & \text{if } z < 0 \\ 0, & \text{if } z = 0 \\ +1, & \text{if } z > 0 \end{cases} \quad (20)$$

In order to perform the integration over the variable  $\varphi$ , the function  $e^{-jk_0 n_\rho \rho \cos(\varphi-\beta)}$  is expressed as a series of Bessel functions [Stratton, 1941],

$$e^{-jk_0 n_\rho \rho \cos(\varphi-\beta)} = \sum_{u=-\infty}^{\infty} (-j)^u J_u(k_0 n_\rho \rho) e^{ju(\varphi-\beta)} \quad (21)$$

and the spatial spectrum of the current is expanded as a Fourier series

$$\begin{aligned} \mathbf{J}(n_\rho, \varphi, n_{z\pm} \text{sgn}(z)) &= \sum_{m=-\infty}^{\infty} \mathbf{d}_{m\pm}(n_\rho) e^{jm\varphi} \\ \mathbf{d}_{m\pm}(n_\rho) &= \frac{1}{2\pi} \int_0^{2\pi} \mathbf{J}(n_\rho, \varphi, n_{z\pm} \text{sgn}(z)) e^{-jm\varphi} d\varphi \end{aligned} \quad (22)$$

For any current distribution the vector coefficients for any integer  $m$  satisfy the relation

$$\mathbf{d}_{m\pm}(-n_\rho) = (-1)^m \mathbf{d}_{m\pm}(n_\rho) \quad (23)$$

This relation is very important and will be used later. The proof is given in Appendix B. Replacing the integrand of

(19) with equations (21) and (22) and integrating over  $\varphi$ , the vector potential becomes

$$\mathbf{A}_{\pm}(\mathbf{r}) = \frac{\mu_0 \omega}{2\pi k_0^3} \sum_{m=-\infty}^{+\infty} (-j)^m e^{jm\beta} \int_0^{\infty} dn_{\rho} \left\{ \frac{n_{\rho} e^{-jk_0 n_{\pm} \operatorname{sgn}(z)z}}{2q_{\pm} n_{z\pm}} \cdot \mathbf{d}_{m\pm}(n_{\rho}) J_m(k_0 n_{\rho} \rho) \right\}. \quad (24)$$

As expected, the vector potential of each mode at any observation point  $\mathbf{r}$  is expressed as a composition of waves that look like plane waves along the ambient magnetic field, and cylindrical waves in the perpendicular direction.

#### 4. Far Field Analysis

[12] An asymptotic expansion is applied to the Bessel function in (24) and only the lowest-order term remains to give the far field since the higher-order terms attenuate more quickly with distance,

$$J_m(k_0 n_{\rho} \rho) = \left( \frac{2}{\pi k_0 n_{\rho} \rho} \right)^{1/2} \cos\left(k_0 n_{\rho} \rho - \frac{m\pi}{2} - \frac{\pi}{4}\right) \quad (25)$$

Substitution into equation (24) yields

$$\mathbf{A}_{\pm}(\mathbf{r}) = \frac{\mu_0 \omega}{2\pi k_0^3} \left( \frac{1}{2\pi k_0 \rho} \right)^{1/2} \sum_{m=-\infty}^{\infty} e^{jm\beta} \left\{ \begin{aligned} & e^{+j\frac{\pi}{4}} \int_0^{\infty} dn_{\rho} \frac{\sqrt{n_{\rho}}}{2q_{\pm} n_{z\pm}} \mathbf{d}_{m\pm}(n_{\rho}) e^{-jk_0(n_{z\pm} \operatorname{sgn}(z)z + n_{\rho} \rho)} \\ & + (-1)^m e^{-j\frac{\pi}{4}} \int_0^{\infty} dn_{\rho} \frac{\sqrt{n_{\rho}}}{2q_{\pm} n_{z\pm}} \mathbf{d}_{m\pm}(n_{\rho}) e^{-jk_0(n_{z\pm} \operatorname{sgn}(z)z - n_{\rho} \rho)} \end{aligned} \right\} \quad (26)$$

Changing the variable  $n_{\rho}$  with  $-n_{\rho}$  in the second integral and noting that for the even functions  $q_{\pm}(-n_{\rho}) = q_{\pm}(n_{\rho})$ ,  $n_{z\pm}(-n_{\rho}) = n_{z\pm}(n_{\rho})$ , and using the relation (23), the two terms can be combined into one integral over the whole real axis of  $n_{\rho}$  from negative to positive infinity,

$$\mathbf{A}_{\pm}(\mathbf{r}) = \frac{\mu_0 \omega}{2\pi k_0^3} \left( \frac{1}{2\pi k_0 \rho} \right)^{1/2} \sum_{m=-\infty}^{\infty} e^{jm\beta} e^{+j\frac{\pi}{4}} \int_{-\infty}^{+\infty} dn_{\rho} \frac{\sqrt{n_{\rho}}}{2q_{\pm} n_{z\pm}} \mathbf{d}_{m\pm}(n_{\rho}) e^{-jk_0 n_s r} \quad (27)$$

where a ‘‘spherical refractive index,  $n_s$ ’’ has been introduced defined by

$$n_s = n_{z\pm} |\cos \alpha| + n_{\rho} \sin \alpha \quad (28)$$

The sign of the square root in (27) is not important since the current is arbitrary anyway. It should be pointed out that in the above derivation two cases have been excluded:  $\alpha = 0$  and  $\alpha = \pi$  ( $\rho = 0$ ) and  $\alpha = \pi/2$  ( $z = 0$ ). For the parallel direction, the Bessel asymptotic in equation (25) does not hold although the vector potential expression as given by equation (24) is valid for this case, and the perpendicular direction is not included in the expression for the general vector potential as shown by equation (19). However, the general vector potential is merely introduced as an intermediate function for the computation of the electromagnetic field and has no direct physical meaning. We have the

freedom to choose the values for these two special cases and define them as the limits of the general solution when  $\alpha \rightarrow 0$  (and  $\alpha \rightarrow \pi$ ) and  $\alpha \rightarrow \pi/2$ . From now on, the asymptotic expression for the general vector potential, equation (27), is valid for any point in the observing coordinate system.

[13] The spherical refractive index defined by equation (28) is a multivalued function representing a four-sheet Riemann surface with eight branch points, where individual sheets join together. Four branch points are determined by  $n_z(n_{\rho}) = 0$ , and the other four by  $q(n_{\rho}) = 0$ . The asymptotic form of the integral in equation (27) can be found using the saddle point method [Felsen and Marcuvitz, 1994]. The integrand function is analytically extended to the whole Riemann surface and the integral path of the real axis is deformed to the steepest descent through the saddle point. The asymptotic form of equation (27) then becomes

$$\begin{aligned} \mathbf{A}_{\pm}(\mathbf{r}) &= \frac{\mu_0 \omega}{2\pi k_0^4} \left[ n_{\rho s} / (n_{z\pm}''(n_{\rho s}) \sin \alpha |\cos \alpha|) \right]^{1/2} \frac{1}{2q_{\pm} n_{z\pm}} \\ &\cdot \left[ \sum_{m=-\infty}^{\infty} e^{jm\beta} \mathbf{d}_{m\pm}(n_{\rho s}) \right] \frac{e^{-jk_0 n_s r}}{r} \\ q_{\pm} &= \left[ (\varepsilon_1 - \varepsilon_3)^2 n_{\rho s}^4 - 4\varepsilon_2^2 \varepsilon_3 n_{\rho s}^2 + 4\varepsilon_2^2 \varepsilon_3^2 \right]^{1/2} \\ &\cdot (-\pi/2 \leq \arg(q_{\pm}) < \pi/2, \pi/2 \leq \arg(q_{\pm}) < 3\pi/2) \\ n_{z\pm} &= \left[ (2\varepsilon_1 \varepsilon_3 - (\varepsilon_1 + \varepsilon_3) n_{\rho s}^2 + q_{\pm}(n_{\rho s})) / (2\varepsilon_3) \right]^{1/2}, \\ n_{z\pm}''(n_{\rho s}) &= \frac{d^2 n_{z\pm}(n_{\rho})}{dn_{\rho}^2} \Big|_{n_{\rho} = n_{\rho s}} \\ n_s &= n_{z\pm} |\cos \alpha| + n_{\rho s} \sin \alpha, \quad (-\pi/2 \leq \arg(n_s) \leq 0) \end{aligned} \quad (29)$$

In equation (29)  $n_s$  is referred to as the refractive index of spherical waves, or simply, the spherical refractive index. And the saddle point,  $n_{\rho s}$ , is the root of the equation  $\frac{dn_s}{dn_{\rho}} = 0$ . From equation (28), it can be written as

$$\begin{aligned} n_{\rho} \left[ -(\varepsilon_1 + \varepsilon_3)q + (\varepsilon_1 - \varepsilon_3)^2 n_{\rho}^2 - 2\varepsilon_2^2 \varepsilon_3 \right] |\cos \alpha| \\ + 2\varepsilon_3 n_{\rho} q \sin \alpha = 0 \end{aligned} \quad (30)$$

Note that equation (29) represents the case when the saddle point equation (30) has only one single root for a given direction and for either  $q_{+}$  or  $q_{-}$  mode. If there is more than one saddle point for a mode, the contributions from all saddle points should be taken into account, and the asymptotic solution is the summation of all contributions.

[14] Recalling Fourier expansion (22), the asymptotic form of the vector potential finally becomes for  $r \rightarrow \infty$ :

$$\begin{aligned} \mathbf{A}_{\pm}(\mathbf{r}) &= \frac{\mu_0 \omega}{2\pi k_0^4} F_{1\pm}(\alpha) \mathbf{J}(n_{\rho s}, \beta, n_{z\pm} \operatorname{sgn}(\pi/2 - \alpha)) \frac{e^{-jk_0 n_s r}}{r} \\ F_{1\pm}(\alpha) &= \frac{1}{2q_{\pm} n_{z\pm}} \left[ n_{\rho s} / (n_{z\pm}''(n_{\rho s}) \sin \alpha |\cos \alpha|) \right]^{1/2}. \end{aligned} \quad (31)$$

[15] The above result is derived using the asymptotic approach. As done by some other authors, equality signs are used in the asymptotic equations (25) to (31). It should be pointed out, that all of them represent the lowest order of the

asymptotic expansion, and they are valid only in the far region as the distance is approaching infinity. Asymptotic results do not imply approximations, however, and the asymptotic form of a function gives its precise value as the argument approaches infinity. In praxis, the “minimum distance” to the far field depends on the anisotropy of the plasma as discussed by *Rasmussen et al.* [1986], but the distances involved in radio sounding with IMAGE/RPI usually far exceed this minimum distance.

## 5. Refractive Index of Spherical Waves

[16] The refractive index is determined by the roots of the saddle point equation (30). Thus the spherical refractive index can be interpreted geometrically as the saddle peak on the Riemann surface. It is clear that the saddle points are symmetric with respect to the perpendicular direction and one need only find the roots for the range  $0 \leq \alpha \leq \pi/2$ .

[17] At first, one can find the roots of equation (30) for special cases. In the parallel direction  $\alpha = 0$ ,  $n_\rho = 0$  is one root giving

$$\begin{aligned} n_{\rho s} &= 0 \\ q_{\pm} &= 2(\varepsilon_2^2 \varepsilon_3^2)^{1/2} \\ n_{z\pm} &= [(2\varepsilon_1 \varepsilon_3 + q_{\pm}) / (2\varepsilon_3)]^{1/2} \\ n_s &= n_{z\pm}, \quad (-\pi/2 \leq \arg(n_s) \leq 0) \end{aligned} \quad (32)$$

In the perpendicular direction  $\alpha = \pi/2$ , the branch point  $n_z = 0$  is one root yielding

$$\begin{aligned} n_{\rho s} &= \sqrt{\varepsilon_3}, \quad \sqrt{(\varepsilon_1^2 - \varepsilon_2^2) / \varepsilon_3} \\ q_{\pm} &= [(\varepsilon_1 - \varepsilon_3)^2 n_{\rho s}^4 - 4\varepsilon_2^2 \varepsilon_3 n_{\rho s}^2 + 4\varepsilon_2^2 \varepsilon_3^2]^{1/2} \\ n_{z\pm} &= 0 \\ n_s &= n_{\rho s}, \quad (-\pi/2 \leq \arg(n_s) \leq 0) \end{aligned} \quad (33)$$

It can be verified that in these two special directions the refractive index of spherical waves is equal to those of plane waves.

[18] Unfortunately, it is difficult to find the roots of equation (30) in an explicit analytical form in other directions, but they can be found numerically. It is more convenient to perform square operations for  $q(n_\rho)$  and  $n_z(n_\rho)$  in equation (30) so that it is transformed to a sextic (sixth-order polynomial) equation

$$\begin{aligned} a_6 \tau^6 + a_5 \tau^5 + a_4 \tau^4 + a_3 \tau^3 + a_2 \tau^2 + a_1 \tau + a_0 &= 0 \\ \tau &= n_\rho^2 \end{aligned} \quad (34)$$

where the expressions of the polynomial coefficients are listed in Appendix C. There are six roots of the polynomial equation (34):  $\tau_i$ , ( $i = 1, 2, \dots, 6$ ). The required saddle points must be included in them and the remaining task is to identify which of them qualify as the saddle points giving physically meaningful solutions.

[19] For collisionless plasma, all the coefficients in (34) are real numbers, and at least two real roots exist and the others are conjugate pairs, if any, for such an even order polynomial equation. The conjugate pairs result in waves with attenuation along the propagation path. This is

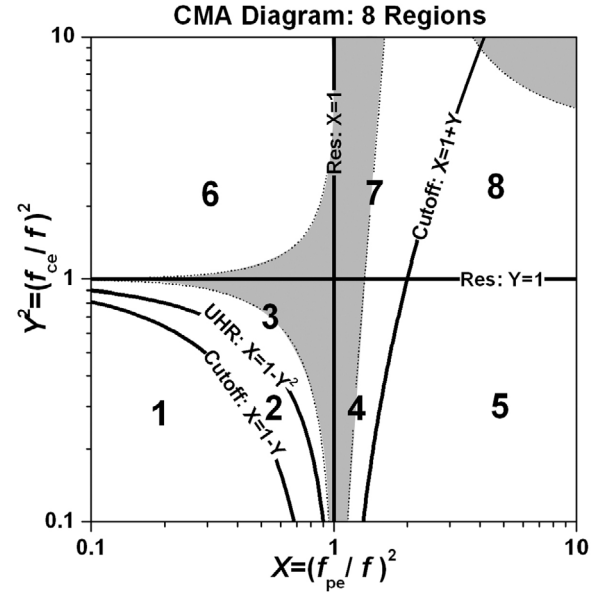


Figure 2. CMA diagram for cold plasma.

physically unreasonable for collision-free plasma and all the roots in conjugate pairs should be abandoned. For any pure real root, either positive or negative, it qualifies if and only if it meets the following two conditions:

[20] 1. The spherical refractive index must be in the fourth quadrant,  $-\pi/2 \leq \arg(n_s) \leq 0$ . This condition is set to ensure that the solution is physically meaningful.

[21] 2. The original equation (30) must be satisfied. This condition is set because the square operations are performed to derive equation (34) from (30), and thus the two equations are not absolutely equivalent: the roots of (30) must be included in the roots of (34) but a root of (34) may not be a root of (30).

[22] The signs of the square root for  $n_\rho = \sqrt{\tau}$ ,  $q(n_\rho)$  and  $n_z(n_\rho)$  in equation (29) should be properly selected so that the above two conditions are satisfied. Once the sign of  $q(n_\rho)$  is determined, the mode type is identified. If none of the sign selections for a root is able to satisfy the above two conditions, then this root is not qualified. It is obvious that, corresponding to a qualified positive or negative root, the spherical refractive index is pure real or pure imaginary, indicating that the spherical wave is either progressive or evanescent in the given direction.

[23] The plasma parameters can be divided into several regions by the resonance and cutoff lines to construct the CMA diagram so as to categorize wave property in density/ambient magnetic field space [Swanson, 1989]. In each CMA region the topological property of the refractive index remains unchanged. For collisionless cold plasma the CMA diagram with eight regions becomes simple, as shown in Figure 2. The solution (31) is valid for any region of the CMA diagram except for the region boarder lines, where wave phenomena cannot be described by the cold plasma approximation.

[24] According to the theory of sextic polynomials with real coefficients, the numbers of positive and negative real roots are determined by the sign of  $a_6 a_0$ : If  $a_6 a_0 > 0$ ,

equation (34) has at least two real roots which are both positive or both negative. If  $a_6 a_0 < 0$ , then one root is positive and the other is negative. It is easy to verify that

$$a_6 a_0 = 0, \text{ If } \begin{cases} \alpha = 0, \text{ for all CMA Regions;} \\ \alpha = \alpha_{\text{SRC}}, \text{ for CMA Regions 3, 7 and 8,} \\ \alpha_{\text{SRC}} = \arctan \sqrt{-\varepsilon_1 / \varepsilon_3}. \end{cases}$$

$$a_6 a_0 > 0, \text{ If } \begin{cases} 0 < \alpha \leq \pi/2, \text{ for CMA Regions 1, 5 and 6;} \\ \alpha_{\text{SRC}} < \alpha \leq \pi/2, \text{ for CMA Region 3;} \\ 0 < \alpha < \alpha_{\text{SRC}}, \text{ for CMA Regions 7 and 8.} \end{cases}$$

$$a_6 a_0 < 0, \text{ If } \begin{cases} 0 < \alpha \leq \pi/2, \text{ for CMA Regions 2 and 4;} \\ 0 < \alpha < \alpha_{\text{SRC}}, \text{ for CMA Region 3;} \\ \alpha_{\text{SRC}} < \alpha \leq \pi/2, \text{ for CMA Regions 7 and 8.} \end{cases} \quad (35)$$

Therefore, both mode waves are progressive in CMA regions 1 and 6, but only one mode wave is progressive in regions 2 and 4, and the other is evanescent. In region 5, the excited waves of both modes are evanescent. It is interesting to note that one progressive mode wave is confined in a cone in regions 3 (extraordinary mode), and 7 and 8 (whistler mode). The cone is referred to as the radiation cone. The cone for the extraordinary wave in region 3 is extended around the direction perpendicular to the ambient magnetic field, and for the whistler it is confined in the cone around the ambient magnetic field. Since the resonance cone angle for plane waves [Stix, 1992] is

$$\alpha_{\text{RC}} = \arctan \sqrt{-\varepsilon_3 / \varepsilon_1} \quad (36)$$

the radiation cone angle,  $\alpha_{\text{SRC}}$ , and the resonance angle,  $\alpha_{\text{RC}}$ , are complementary, i.e.,

$$\alpha_{\text{SRC}} + \alpha_{\text{RC}} = \pi/2 \quad (37)$$

When crossing the border of the radiation cone, the refractive index of spherical waves jumps from a positive real number to a negative imaginary number. Typical refractive indices of spherical waves for collisionless plasma are plotted in Figure 3, the real parts in red, the imaginary parts in green. For comparison the refractive indices of plane waves (dotted lines) for the same plasma parameters are also plotted in Figure 3.

[25] As shown in Figure 3, in the directions parallel and perpendicular to the ambient magnetic field, the spherical index is equal to the plane wave refractive index. In all other directions they are different. This difference is small for very weak plasma, but becomes larger with increasing anisotropy. In regions 1 and 6, there are two modes of progressive waves. In regions 2 and 4, only one mode wave is progressive. In region 5, there are no progressive waves excited. In region 3 both modes are progressive but one is confined to a cone around the perpendicular direction. In region 7, there is a progressive mode wave excited in addition to the whistler wave. The whistler mode waves are also excited in region 8. The whistlers are confined to the radiation cone.

[26] In general, (34) has only two real roots providing the qualified saddle points for the two modes. However, there are some cases where multiple real roots exist and it remains to be determined whether all the real roots are qualified saddle points. In the parallel direction,  $\alpha = 0$ , equation (30) reduces to

$$n_\rho [-(\varepsilon_1 + \varepsilon_3)q(n_\rho) + (\varepsilon_1 - \varepsilon_3)^2 n_\rho^2 - 2\varepsilon_2^2 \varepsilon_3] = 0 \quad (38)$$

In addition to the root  $n_\rho = 0$ , there are two additional roots,

$$n_\rho^2 = \frac{2\varepsilon_1 \varepsilon_2^2 \varepsilon_3 \pm \sqrt{\Delta}}{\varepsilon_1 (\varepsilon_1 - \varepsilon_3)^2},$$

$$\Delta \equiv \varepsilon_1 \varepsilon_2^2 \varepsilon_3 (\varepsilon_1 + \varepsilon_3)^2 (\varepsilon_2 + \varepsilon_1 - \varepsilon_3) (\varepsilon_2 - \varepsilon_1 + \varepsilon_3) \quad (39)$$

In the case of  $\Delta \geq 0$ , these two roots are real and one of them is equal to zero provided that

$$X = 2 \frac{1 - Y}{2 - Y} \equiv X_1$$

$$X = 2 \frac{1 + Y}{2 + Y} \equiv X_2 \quad (40)$$

It turns out that for directions close to the magnetic field direction, and not only parallel to the field, there exist two additional real roots, and they qualify as progressive wave solutions, indicating the existence of submodes: a “-” mode in CMA region 4 if  $1 < X < X_2$ , a “+” mode if  $X < X_2$  in region 7, and a “-” mode if  $X > X_1$  and  $Y > 2$  in regions 7 and 8.

[27] In the perpendicular direction, equation (30) shows that the coupling points, from  $q(n_\rho) = 0$ , are roots in addition to the roots from  $n_z(n_\rho) = 0$ . It can be proved that around the perpendicular direction for the “-” mode in CMA region 3 two more progressive waves exist if  $X_3 < X < 1$  where

$$X_3 = \sqrt{1 - Y^2} \quad (41)$$

The areas in which submodes exist are shaded in the CMA diagram in Figure 2. The border lines are defined by equations (40) and (41). Submode waves for the “+” mode also exist in region 6, but we were unable to find the analytical expression for the border line and had to use the results of numerical computations.

[28] Several examples for the spherical refractive indices with submodes are plotted in Figure 4. The plane wave refractive indices are also plotted in Figure 4 for comparison. When submodes exist, more than one spherical wave with different propagation speeds will be excited in a given direction, but there is always only one plane wave. When the plasma parameters cross a border line entering the shaded area in the CMA diagram, submode waves start to occur extending the range of the polar angle. The farther the parameters depart from the border line, the larger the range. Submodes also exist in some cases for evanescent spherical

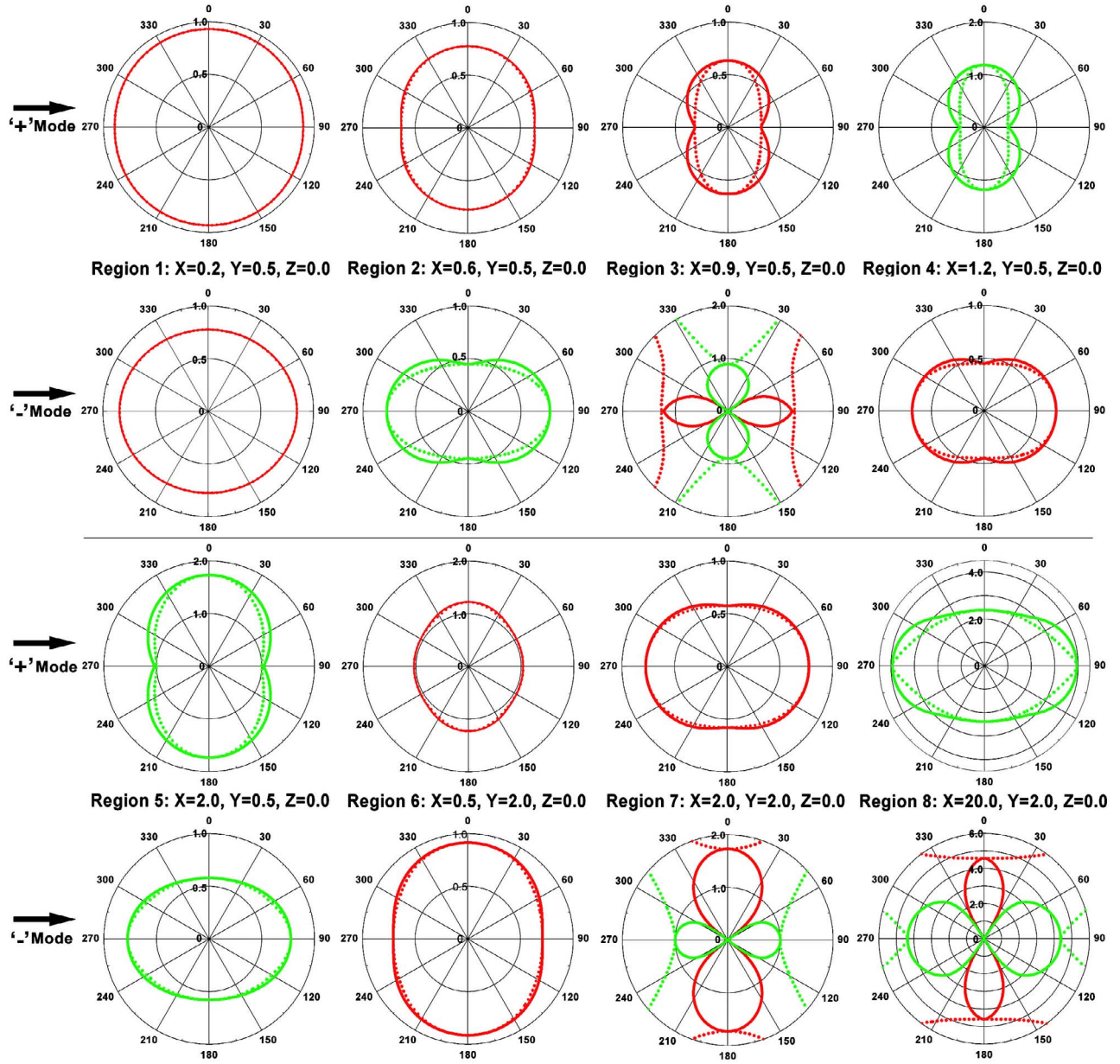


**Figure 3.** Real (red) and imaginary (green) parts of the refractive indices for typical plasma parameters (solid lines, spherical waves; dotted lines, plane waves).

waves, but they are not discussed here since they are of no physical importance.

## 6. Spherical Waves in the Far Field

[29] The excited electromagnetic field in the far region is derived from equation (12). At first, the components in the Cartesian coordinate systems are derived and then transformed into the spherical coordinate system. In the course of the derivation, attention is paid to the far field, and thus all the terms with higher orders of attenuation with distance can be ignored. If the subscripts ( $x, y, z$ ) are replaced by (1, 2, 3),

the components of the electric field in equation (12) are written as

$$E_{i\pm}(\mathbf{r}) = \sum_{j=1}^3 \Lambda_{ij} A_{j\pm}(\mathbf{r}), \quad (i = 1, 2, 3) \quad (42)$$

where  $A_{j\pm}(\mathbf{r})$  are the components of the vector potential,

$$A_{j\pm}(\mathbf{r}) = \frac{\mu_0 \omega}{2\pi k_0^4} F_{1\pm}(\alpha) J_{\pm}(n_{ps}, \beta, n_{z\pm} \operatorname{sgn}(\pi/2 - \alpha)) \frac{e^{-jk_0 n_s r}}{r}, \quad (j = 1, 2, 3) \quad (43)$$

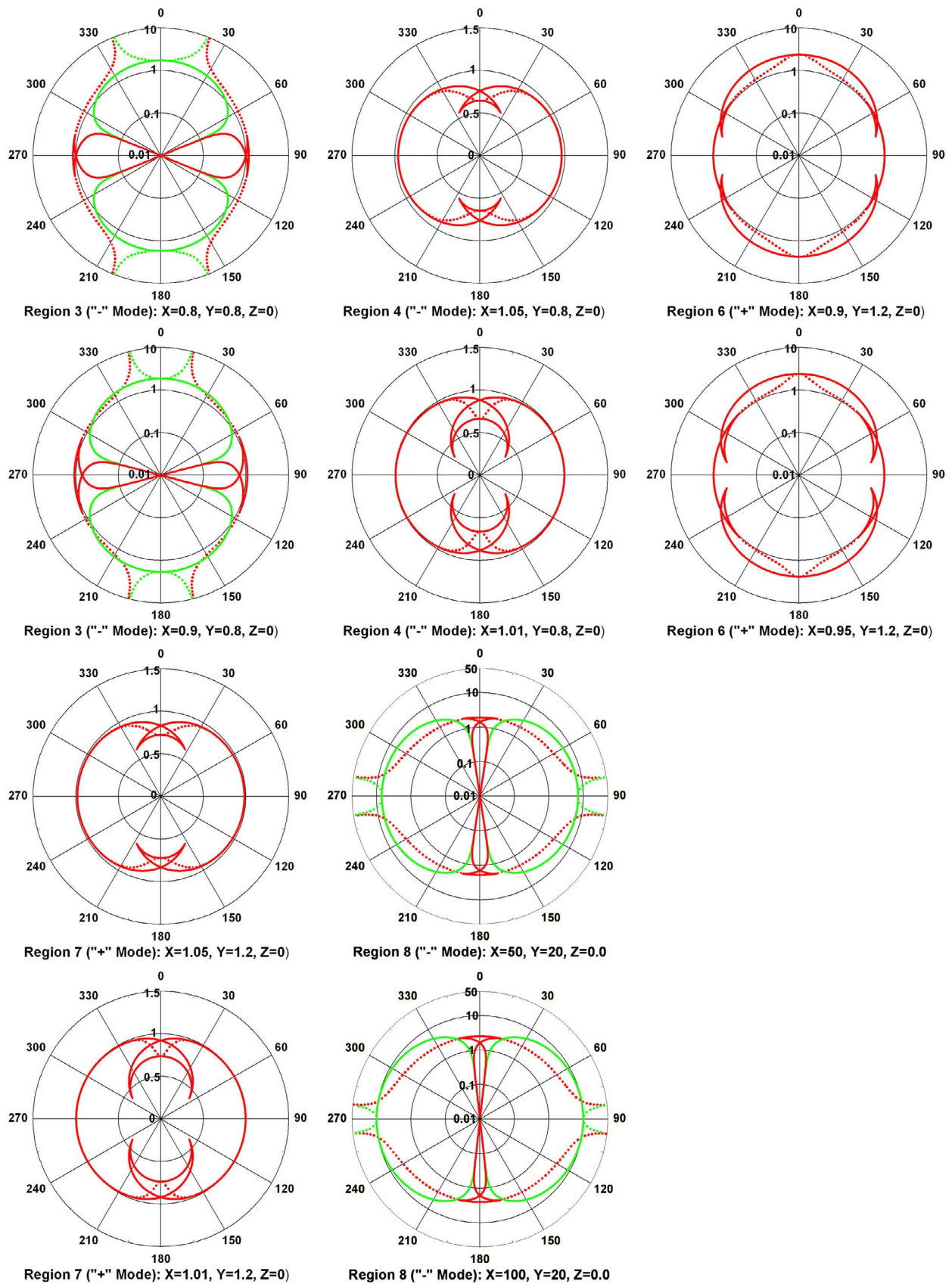


**Figure 4.** Progressive submode waves in CMA regions 3, 4, 6, 7, and 8: real (red) and imaginary (green) parts of the refractive indices (solid lines, spherical waves; dotted lines, plane waves).

Since the vector potential components are expressed in spherical coordinates while the differential operator is given in Cartesian coordinates, one need to use the Jacobian for the coordinate transformation in computation. As examples, the partial derivatives of the first order for  $A_{x\pm}(\mathbf{r})$  are derived,

$$\begin{aligned} \frac{\partial}{\partial x} A_{x\pm}(\mathbf{r}) &= \left\{ \begin{array}{l} \sin \alpha \cos \beta \left( -jk_0 n_s - \frac{1}{r} \right) \\ + \frac{1}{r} \cos \alpha \cos \beta \left( \frac{1}{F_{1\pm}(\alpha)} \frac{\partial F_{1\pm}(\alpha)}{\partial \alpha} + \frac{1}{J_{x\pm}(\alpha, \beta)} \frac{\partial J_{x\pm}(\alpha, \beta)}{\partial \alpha} - jk_0 r \frac{dn_s}{d\alpha} \right) \\ - \frac{\sin \beta}{r \sin \alpha J_{x\pm}(\alpha, \beta)} \frac{\partial J_{x\pm}(\alpha, \beta)}{\partial \beta} \end{array} \right\} A_{x\pm}(\mathbf{r}) \\ \frac{\partial}{\partial y} A_{x\pm}(\mathbf{r}) &= \left\{ \begin{array}{l} \sin \alpha \sin \beta \left( -jk_0 n_s - \frac{1}{r} \right) \\ + \frac{1}{r} \cos \alpha \sin \beta \left( \frac{1}{F_{1\pm}(\alpha)} \frac{\partial F_{1\pm}(\alpha)}{\partial \alpha} + \frac{1}{J_{x\pm}(\alpha, \beta)} \frac{\partial J_{x\pm}(\alpha, \beta)}{\partial \alpha} - jk_0 r \frac{dn_s}{d\alpha} \right) \\ + \frac{\cos \beta}{r \sin \alpha J_{x\pm}(\alpha, \beta)} \frac{\partial J_{x\pm}(\alpha, \beta)}{\partial \beta} \end{array} \right\} A_{x\pm}(\mathbf{r}) \\ \frac{\partial}{\partial z} A_{x\pm}(\mathbf{r}) &= \left\{ \cos \alpha \left( -jk_0 n_s - \frac{1}{r} \right) - \frac{\sin \alpha}{r} \left( \frac{1}{F_{1\pm}(\alpha)} \frac{\partial F_{1\pm}(\alpha)}{\partial \alpha} + \frac{1}{J_{x\pm}(\alpha, \beta)} \frac{\partial J_{x\pm}(\alpha, \beta)}{\partial \alpha} - jk_0 r \frac{dn_s}{d\alpha} \right) \right\} A_{x\pm}(\mathbf{r}) \end{aligned} \quad (44)$$

Since we are mainly interested in the far field, the faster attenuating terms with higher orders of  $1/r$  can be dropped and the above partial derivatives become

$$\begin{aligned} \frac{\partial}{\partial x} A_{x\pm}(\mathbf{r}) &= -jk_0 \cos \beta \left( n_s \sin \alpha + \cos \alpha \frac{dn_s}{d\alpha} \right) A_{x\pm}(\mathbf{r}) \\ \frac{\partial}{\partial y} A_{x\pm}(\mathbf{r}) &= -jk_0 \sin \beta \left( n_s \sin \alpha + \cos \alpha \frac{dn_s}{d\alpha} \right) A_{x\pm}(\mathbf{r}) \\ \frac{\partial}{\partial z} A_{x\pm}(\mathbf{r}) &= -jk_0 \left( n_s \cos \alpha - \sin \alpha \frac{dn_s}{d\alpha} \right) A_{x\pm}(\mathbf{r}) \end{aligned} \quad (45)$$

The refractive index of spherical waves defined by (29) is a function of  $n_{\rho s}$  and  $\alpha$ , and  $n_{\rho s}$  itself is also a function of  $\alpha$ . Then we have

$$\begin{aligned} \frac{dn_s}{d\alpha} &= \frac{\partial n_z}{\partial n_{\rho s}} \frac{dn_{\rho s}}{d\alpha} \operatorname{sgn} \left( \frac{\pi}{2} - \alpha \right) \cos \alpha - n_z \operatorname{sgn} \left( \frac{\pi}{2} - \alpha \right) \sin \alpha \\ &+ \sin \alpha \frac{dn_{\rho s}}{d\alpha} + n_{\rho s} \cos \alpha \end{aligned} \quad (46)$$

Since  $n_{\rho s}$  for either wave mode is a root of the saddle point equation (30), equation (46) is simplified to

$$\frac{dn_s}{d\alpha} = -n_z \operatorname{sgn}(\pi/2 - \alpha) \sin \alpha + n_{\rho s} \cos \alpha \quad (47)$$

Then equation (45) becomes

$$\begin{aligned} \frac{\partial}{\partial x} A_{x\pm}(\mathbf{r}) &= -jk_0 n_{\rho s} \cos(\beta) A_{x\pm}(\mathbf{r}) \\ \frac{\partial}{\partial y} A_{x\pm}(\mathbf{r}) &= -jk_0 n_{\rho s} \sin(\beta) A_{x\pm}(\mathbf{r}) \\ \frac{\partial}{\partial z} A_{x\pm}(\mathbf{r}) &= -jk_0 \|n_z\| A_{x\pm}(\mathbf{r}) \end{aligned} \quad (48)$$

where we introduced the notation  $\|n_z\|$

$$\|n_z\| \equiv n_z \operatorname{sgn}(\pi/2 - \alpha). \quad (49)$$

The derivatives for the other two components  $A_{y\pm}(\mathbf{r})$  and  $A_{z\pm}(\mathbf{r})$  are in the same form as (48). This result shows that, in order to find the far field, the computational rule to find the

derivatives of the vector potential can simply be expressed as factors,

$$\begin{aligned} \frac{\partial}{\partial x} &\Rightarrow -jk_0 n_{\rho s} \cos \beta \\ \frac{\partial}{\partial y} &\Rightarrow -jk_0 n_{\rho s} \sin \beta \\ \frac{\partial}{\partial z} &\Rightarrow -jk_0 \|n_z\| \end{aligned} \quad (50)$$

As concerns the far field, this computational rule can be applied to the derivatives of higher orders so that the elements of the differential operator in equation (42) can all be expressed as factors (see Appendix D).

[30] In the Cartesian coordinate system, the components of the electric field in (42) can easily be obtained. The computational rule (50) can also be applied to the differential operator  $\nabla \times$  (the curl) in equation (12) to derive the magnetic field. The far field expressed in the spherical coordinate system is most useful and it can easily be derived through coordinate transformation. The expressions of the components of the far field are found in Appendix D. These expressions are lengthy, however, the far field can be written in a simple form as

$$\begin{aligned} \mathbf{E}(r, \alpha, \beta) &= \mathbf{E}_+(r, \alpha, \beta) + \mathbf{E}_-(r, \alpha, \beta), \\ \mathbf{E}_{\pm}(r, \alpha, \beta) &= \mathbf{E}_{0\pm}(\alpha, \beta; \varepsilon) \frac{e^{-jk_0 n_s r}}{r} \\ \mathbf{H}(r, \alpha, \beta) &= \mathbf{H}_+(r, \alpha, \beta) + \mathbf{H}_-(r, \alpha, \beta), \\ \mathbf{H}_{\pm}(r, \alpha, \beta) &= \mathbf{H}_{0\pm}(\alpha, \beta; \varepsilon) \frac{e^{-jk_0 n_s r}}{r} \end{aligned} \quad (51)$$

The phasors  $\mathbf{E}_{0\pm}(\alpha, \beta; \varepsilon)$  and  $\mathbf{H}_{0\pm}(\alpha, \beta; \varepsilon)$  depend on the current source, the direction, and the plasma parameters.

[31] As indicated by equation (24), each mode is a superposition of waves, which look like plane waves along the ambient magnetic field and cylindrical waves in the

**Table 1.** Polarization Type of Spherical Waves

	“+” Mode	“-” Mode
Region 1	L	R
Region 2	L	/
Region 3	L	R <sup>a</sup>
Region 4	/	L
Region 5	/	/
Region 6	R	L
Region 7	L	R
Region 8	/	R

<sup>a</sup>After crossing the coupling point  $q = 0$ , the polarization for the submode waves changes to L type.

perpendicular direction, and these waves interfere with each other to form the far field. Now as revealed by (51), the interference results in a reconstruction of waves in the far region for each mode, which looks like a spherical wave as the amplitude is decreasing inversely proportional to distance; however the propagation speed varies with the polar angle so that the wavefront is actually not a sphere, its shape is characterized by the anisotropic medium.

[32] It should be pointed out that there is, in general, a nonzero field component in the radial direction but the major components are transverse. The polarization for the two transverse components of a progressive wave is described by a polarization factor [Budden, 1985]

$$\mathcal{T}_{\pm}(\alpha, \beta) = \frac{E_{\alpha\pm}(r, \alpha, \beta)}{E_{\beta\pm}(r, \alpha, \beta)} \quad (52)$$

The polarization factor contains the information of amplitude ratio and phase difference of the two transverse components. It is generally a complex number representing elliptical polarization. The sign of the imaginary part determines the rotating direction. The vector of the electric field is rotating in the left (L) or right (R) hand direction. Because of the symmetrical property of the far field, the polarization remains unchanged with respect to the direction of the ambient magnetic field.

[33] It is found that the polarization of left or right hand rotation is the same as plane wave propagation in the same direction. The polarization types for progressive modes for the eight CMA regions are summarized in Table 1.

[34] The excited electromagnetic wave carries energy from the current source to the far region. The Poynting vector describes the flow direction and power density. The time average of the Poynting vector is

$$\mathbf{S} = \frac{1}{2} \text{Re}(\mathbf{E} \times \mathbf{H}^*) \quad (53)$$

where  $(\mathbf{E}, \mathbf{E}^*)$  and  $(\mathbf{H}, \mathbf{H}^*)$  denote conjugate pairs. Since the far field can be decomposed into two mode waves which propagate independently, the Poynting vectors for the two modes in spherical coordinates take the form

$$\begin{aligned} \mathbf{S}_+(r, \alpha, \beta) &= (S_{r+}(r, \alpha, \beta), S_{\alpha+}(r, \alpha, \beta), S_{\beta+}(r, \alpha, \beta)) \\ \mathbf{S}_-(r, \alpha, \beta) &= (S_{r-}(r, \alpha, \beta), S_{\alpha-}(r, \alpha, \beta), S_{\beta-}(r, \alpha, \beta)) \end{aligned} \quad (54)$$

There is no difficulty deriving these expressions for the components using the information given in Appendix D.

[35] It is very interesting and important to note that the two transverse components of  $S$  for either mode are exactly equal to zero,

$$\begin{aligned} S_{\alpha\pm}(r, \alpha, \beta) &= 0 \\ S_{\beta\pm}(r, \alpha, \beta) &= 0 \end{aligned} \quad (55)$$

indicating that the energy is always flowing along the radial direction parallel to the wave normal. This is different from the plane wave description for anisotropic medium where the wave normal and the energy flow are generally in different directions making the problem more complicated than the isotropic case. The directional agreement of the phase and group velocities of the excited spherical waves makes the anisotropic plasma look like an isotropic medium except that the refractive index changes with the angle from the ambient magnetic field. The analytical proof of equation (55) uses the saddle point equation (30) which specifies the qualitative relation for  $n_{\rho s}$ ,  $q$  and  $n_z$  appearing in the expressions of  $S_{\alpha\pm}(r, \alpha, \beta)$  and  $S_{\beta\pm}(r, \alpha, \beta)$ . The algebraic proof is omitted here since it is too lengthy.

## 7. Convergence to the Isotropic/Free Space Solutions

[36] When the operating frequency is very high as compared to the plasma frequency, or when the ambient magnetic field is very weak, the anisotropy of the plasma diminishes making the medium near isotropic. If the plasma density is very small it will look like free space. In this section the behavior of the derived expressions of the excited far field is examined for the limits  $Y \rightarrow 0$  and/or  $X \rightarrow 0$ , revealing the convergence of the derived magnetoplasma solution to the isotropic/free space case.

[37] For very weak magnetized collisionless plasma, the parameters in equation (1) can be expressed by a Taylor approximation,

$$\begin{aligned} \varepsilon_1 &= \varepsilon_3 - XY^2 + O(Y^4) \\ \varepsilon_2 &= XY + O(Y^3) \\ \varepsilon_3 &= 1 - X \end{aligned} \quad (56)$$

where  $O(Y^m)$ , for example  $O(Y^4)$ , indicates that the omitted lowest-order term is  $\sim Y^m$ . As a result one can find the approximations for the mode discriminator

$$q = \pm 2(\varepsilon_3^2 - \varepsilon_3 n_{\rho}^2)^{1/2} XY + O(Y^2). \quad (57)$$

And for the function

$$n_z = (\varepsilon_3 - n_{\rho}^2)^{1/2} + \frac{-\varepsilon_3 n_{\rho}^2 \pm 2X(\varepsilon_3^2 - \varepsilon_3 n_{\rho}^2)^{1/2}}{4\varepsilon_3(\varepsilon_3 - n_{\rho}^2)^{1/2}} Y + O(Y^2). \quad (58)$$

This gives the derivatives

$$n_z' = \frac{-n_\rho}{(\varepsilon_3 - n_\rho^2)^{1/2}} + \frac{\left\{ -\left[ 2\varepsilon_3(\varepsilon_3^2 - \varepsilon_3 n_\rho^2)^{1/2} \pm 2\varepsilon_3 X \right] (\varepsilon_3 - n_\rho^2) \right\} n_\rho Y}{4\varepsilon_3(\varepsilon_3 - n_\rho^2)^{3/2} (\varepsilon_3^2 - \varepsilon_3 n_\rho^2)^{1/2}} + O(Y^2)$$

$$n_z'' = \frac{-\varepsilon_3}{(\varepsilon_3 - n_\rho^2)^{3/2}} + O(Y) \quad (59)$$

Then the saddle points for the two modes can be found from the equation  $n_z' = -\sin \alpha / |\cos \alpha|$ , i.e.,

$$\frac{-n_\rho}{(\varepsilon_3 - n_\rho^2)^{1/2}} + \frac{\left\{ -\left[ 2\varepsilon_3(\varepsilon_3^2 - \varepsilon_3 n_\rho^2)^{1/2} \pm 2\varepsilon_3 X \right] (\varepsilon_3 - n_\rho^2) \right\} n_\rho Y}{4\varepsilon_3(\varepsilon_3 - n_\rho^2)^{3/2} (\varepsilon_3^2 - \varepsilon_3 n_\rho^2)^{1/2}} + O(Y^2) = -\frac{\sin \alpha}{|\cos \alpha|} \quad (60)$$

Therefore the Taylor expansion of the saddle point takes the form

$$n_{\rho s} = \sqrt{\varepsilon_3} \sin \alpha + \frac{\sin \alpha}{4\varepsilon_3^{3/2}} \left[ -\varepsilon_3^2 (1 + |\cos \alpha|^2) \pm 2X^2 |\cos \alpha| \right] Y + O(Y^2) \quad (61)$$

leading to

$$q_\pm = \pm 2\varepsilon_3 |\cos \alpha| XY + O(Y^2)$$

$$n_{z\pm} = \varepsilon_3^{1/2} |\cos \alpha| - \frac{\sin^2 \alpha}{4\varepsilon_3^{1/2}} \left[ -\varepsilon_3^2 (1 + \cos^2 \alpha) \pm 2|\cos \alpha| X \right] \cdot Y \pm \frac{XY}{2\varepsilon_3^{1/2}} + O(Y^2) n_s = \varepsilon_3^{1/2} + O(Y)$$

$$n_{z\pm}''(n_{\rho s}) = \frac{-1}{\varepsilon_3^{1/2} |\cos \alpha|^3} + O(Y) \quad (62)$$

Now it is easy to find the limits when  $Y \rightarrow 0$ :

$$\begin{aligned} n_{\rho s} &\rightarrow \sqrt{\varepsilon_3} \sin \alpha \\ q_\pm &\rightarrow 0 \\ n_{z\pm} &\rightarrow \sqrt{\varepsilon_3} |\cos \alpha| \\ n_s &\rightarrow \sqrt{\varepsilon_3} \end{aligned} \quad (63)$$

The limit of  $q_\pm \rightarrow 0$  indicates that when  $Y \rightarrow 0$ , there is no mode splitting and the limiting spherical refractive index,  $\sqrt{\varepsilon_3}$ , is equal to that of isotropic plasma. The wave is progressive in all directions if  $X < 1$ , and evanescent if  $X > 1$ . Furthermore, the refractive index approaches one for free space as  $X \rightarrow 0$ .

[38] One needs to take more care in finding the limits for the far field because  $q_\pm$  appears in the denominator of  $F_{1\pm}(\alpha)$ , and the components of the far field given in Appendix D become indeterminate. No attempt is made here to give the detailed derivation; instead we simply summarize the results. Using equations (56) to (62) and applying L'Hopital's rules to the indeterminate terms, one finds that the radial components of the far field approach zero and the two mode waves represent two transverse spherical waves, circularly polarized with equal amplitudes and opposite sense of rotation. Since the refractive indices of the two modes approach the same quantity in the limit, the sum of the two modes results in a linear polarized wave. The limiting expressions are exactly identical to the isotropic/free space solutions.

## 8. Summary and Discussions

[39] Our theoretical investigation of the waves excited by any current source embedded in an unbounded uniform cold magnetoplasma finds that the waves look similar to spherical waves although the speed varies with direction. The refractive index of spherical waves is introduced to describe the phase speed and it differs from that of plane waves, especially for strongly magnetized plasma. Under some conditions, submode spherical waves exist in a given direction. The expressions for the excited far field are derived and the results converge to isotropic/free space solutions. It is found that the polarization type for the spherical wave is generally the same as the plane wave. The energy flow of the spherical wave is always in the radial direction.

[40] In the course of study, it is found that the cylindrical coordinate system is more convenient than the spherical coordinate system for the evaluation of the general vector potential. The spatial spectrum of the current is expanded as a Fourier series instead of a Taylor series because the former generally converges uniformly so that the operation order of summation and integration can be interchanged. Owing to the successful application of the asymptotic approach, the differential operator matrix can be expressed in factors. All these considerations are critical for the successful derivation of the rigorous expressions for the excited far field.

[41] The derived results are valid for any plasma parameters as long as the cold plasma approximation holds. The assumption of uniformity will limit, but not be critical to, the application of the developed results to wave propagation, for example, in the ionosphere-Earth waveguide [Rybachek, 1995; Rybachek *et al.*, 1997], or hemispheric field-aligned propagation in the magnetosphere [Fung and Green, 2005]. We expect, however, that the demonstrated directional agreement of the phase and group velocities of the spherical waves will simplify the ray tracing in a layered anisotropic medium, reducing it to an isotropic task.

[42] The current source in this paper is arbitrary; it may be a current along an antenna, a current induced by lightning or electric jet in space, etc. For radio sounding, the derived results provide another theoretical tool to analyze observed wave phenomena. Radiation properties such as radiation pattern and resistance can be derived with an assumed

current distribution along an antenna. These topics are beyond the scope of this paper.

## Appendix A: Elements of the Differential Operator

[43] The expressions for the elements of the differential operator are

$$\begin{aligned}
A_{11} &= \frac{\partial^2}{\partial x^2} \left( \frac{\partial^2}{\partial x^2} + \frac{\partial^2}{\partial y^2} + \frac{\partial^2}{\partial z^2} \right) + k_0^2 \left( \varepsilon_1 \left( \frac{\partial^2}{\partial x^2} + \frac{\partial^2}{\partial y^2} \right) \right. \\
&\quad \left. + \varepsilon_3 \left( \frac{\partial^2}{\partial x^2} + \frac{\partial^2}{\partial z^2} \right) \right) + \varepsilon_1 \varepsilon_3 k_0^4 \\
A_{12} &= \frac{\partial^2}{\partial x \partial y} \left( \frac{\partial^2}{\partial x^2} + \frac{\partial^2}{\partial y^2} + \frac{\partial^2}{\partial z^2} \right) + k_0^2 \left( \varepsilon_3 \frac{\partial^2}{\partial x \partial y} \right. \\
&\quad \left. + j \varepsilon_2 \left( \frac{\partial^2}{\partial x^2} + \frac{\partial^2}{\partial y^2} \right) \right) + j \varepsilon_2 \varepsilon_3 k_0^4 \\
A_{13} &= \frac{\partial^2}{\partial x \partial z} \left( \frac{\partial^2}{\partial x^2} + \frac{\partial^2}{\partial y^2} + \frac{\partial^2}{\partial z^2} \right) + k_0^2 \left( \varepsilon_1 \frac{\partial^2}{\partial x \partial z} + j \varepsilon_2 \frac{\partial^2}{\partial y \partial z} \right) \\
A_{21} &= \frac{\partial^2}{\partial y \partial x} \left( \frac{\partial^2}{\partial x^2} + \frac{\partial^2}{\partial y^2} + \frac{\partial^2}{\partial z^2} \right) + k_0^2 \left( \varepsilon_3 \frac{\partial^2}{\partial x \partial y} - j \varepsilon_2 \left( \frac{\partial^2}{\partial x^2} + \frac{\partial^2}{\partial y^2} \right) \right) \\
&\quad - j \varepsilon_2 \varepsilon_3 k_0^4 \\
A_{22} &= \frac{\partial^2}{\partial y^2} \left( \frac{\partial^2}{\partial x^2} + \frac{\partial^2}{\partial y^2} + \frac{\partial^2}{\partial z^2} \right) + k_0^2 \left( \varepsilon_1 \left( \frac{\partial^2}{\partial x^2} + \frac{\partial^2}{\partial y^2} \right) \right. \\
&\quad \left. + \varepsilon_3 \left( \frac{\partial^2}{\partial y^2} + \frac{\partial^2}{\partial z^2} \right) \right) + \varepsilon_1 \varepsilon_3 k_0^4 \\
A_{23} &= \frac{\partial^2}{\partial y \partial z} \left( \frac{\partial^2}{\partial x^2} + \frac{\partial^2}{\partial y^2} + \frac{\partial^2}{\partial z^2} \right) + k_0^2 \left( \varepsilon_1 \frac{\partial^2}{\partial y \partial z} - j \varepsilon_2 \frac{\partial^2}{\partial x \partial z} \right) \\
A_{31} &= \frac{\partial^2}{\partial z \partial x} \left( \frac{\partial^2}{\partial x^2} + \frac{\partial^2}{\partial y^2} + \frac{\partial^2}{\partial z^2} \right) + k_0^2 \left( \varepsilon_1 \frac{\partial^2}{\partial x \partial z} - j \varepsilon_2 \frac{\partial^2}{\partial y \partial z} \right) \\
A_{32} &= \frac{\partial^2}{\partial z \partial y} \left( \frac{\partial^2}{\partial x^2} + \frac{\partial^2}{\partial y^2} + \frac{\partial^2}{\partial z^2} \right) + k_0^2 \left( \varepsilon_1 \frac{\partial^2}{\partial y \partial z} + j \varepsilon_2 \frac{\partial^2}{\partial x \partial z} \right) \\
A_{33} &= \frac{\partial^2}{\partial z^2} \left( \frac{\partial^2}{\partial x^2} + \frac{\partial^2}{\partial y^2} + \frac{\partial^2}{\partial z^2} \right) + k_0^2 \left( \varepsilon_1 \left( \frac{\partial^2}{\partial x^2} + \frac{\partial^2}{\partial y^2} + \frac{\partial^2}{\partial z^2} \right) \right. \\
&\quad \left. + (\varepsilon_1^2 - \varepsilon_2^2) k_0^4 \right) \tag{A1}
\end{aligned}$$

## Appendix B: Coefficients of the Fourier Expansion

[44] For any spatial spectrum function  $\mathbf{J}(n_\rho, \varphi, n_{z\pm})$ , the separation into two parts is always possible: the even and odd symmetrical parts with respect to the variable  $n_{z\pm}$ ,

$$\begin{aligned}
\mathbf{J}(n_\rho, \varphi, n_{z\pm}) &= \mathbf{J}_E(n_\rho, \varphi, n_{z\pm}) + \mathbf{J}_O(n_\rho, \varphi, n_{z\pm}) \\
\mathbf{J}_E(n_\rho, \varphi, n_{z\pm}) &= \frac{\mathbf{J}(n_\rho, \varphi, n_{z\pm}) + \mathbf{J}(n_\rho, \varphi, -n_{z\pm})}{2} \\
\mathbf{J}_O(n_\rho, \varphi, n_{z\pm}) &= \frac{\mathbf{J}(n_\rho, \varphi, n_{z\pm}) - \mathbf{J}(n_\rho, \varphi, -n_{z\pm})}{2}
\end{aligned} \tag{B1}$$

Since

$$\begin{aligned}
\mathbf{J}_E(n_\rho, \varphi, -n_{z\pm}) &= \mathbf{J}_E(n_\rho, \varphi, +n_{z\pm}) \\
\mathbf{J}_O(n_\rho, \varphi, -n_{z\pm}) &= -\mathbf{J}_O(n_\rho, \varphi, +n_{z\pm})
\end{aligned} \tag{B2}$$

it is easy to find the relation

$$\mathbf{J}(n_\rho, \varphi, n_{z\pm} \operatorname{sgn}(z)) = \mathbf{J}_E(n_\rho, \varphi, n_{z\pm}) + \operatorname{sgn}(z) \mathbf{J}_O(n_\rho, \varphi, n_{z\pm}) \tag{B3}$$

The coefficients in the Fourier expansion in equation (22) in section 3 can, therefore, be written as

$$\begin{aligned}
\mathbf{d}_{m\pm}(n_\rho) &= \frac{1}{2\pi} \int_0^{2\pi} [\mathbf{J}_E(n_\rho, \varphi, n_{z\pm}) + \operatorname{sgn}(z) \mathbf{J}_O(n_\rho, \varphi, n_{z\pm})] e^{-jm\varphi} d\varphi \\
&= \mathbf{d}_{m\pm}^E(n_\rho) + \operatorname{sgn}(z) \mathbf{d}_{m\pm}^O(n_\rho)
\end{aligned} \tag{B4}$$

Noting that for the even function  $n_{z\pm}(-n_\rho) = n_{z\pm}(n_\rho)$  and using the conversion relations between cylindrical and Cartesian coordinate systems  $n_x = n_\rho \cos \varphi$ ,  $n_y = n_\rho \sin \varphi$  and  $n_z = n_{z\pm}$ , the expression for  $\mathbf{d}_{m\pm}(-n_\rho)$  is derived,

$$\begin{aligned}
\mathbf{d}_{m\pm}(-n_\rho) &= \frac{1}{2\pi} \int_0^{2\pi} [\mathbf{J}_E(-n_\rho, \varphi, n_{z\pm}(-n_\rho)) \\
&\quad + \operatorname{sgn}(z) \mathbf{J}_O(-n_\rho, \varphi, n_{z\pm}(-n_\rho))] e^{-jm\varphi} d\varphi \\
&= \frac{1}{2\pi} \int_0^{2\pi} \left[ \mathbf{J}_E(-n_\rho \cos \varphi, -n_\rho \sin \varphi, n_{z\pm}(-n_\rho)) \right. \\
&\quad \left. + \operatorname{sgn}(z) \mathbf{J}_O(-n_\rho \cos \varphi, -n_\rho \sin \varphi, n_{z\pm}(-n_\rho)) \right] \\
&\quad \cdot e^{-jm\varphi} d\varphi \\
&= \frac{1}{2\pi} \int_0^{2\pi} [\mathbf{J}_E(n_\rho, \varphi - \pi, n_{z\pm}(n_\rho)) \\
&\quad + \operatorname{sgn}(z) \mathbf{J}_O(n_\rho, \varphi - \pi, n_{z\pm}(n_\rho))] e^{-jm\varphi} d\varphi \tag{B5}
\end{aligned}$$

With variable change  $\tau = \varphi - \pi$ , equation (B5) becomes

$$\begin{aligned}
\mathbf{d}_{m\pm}(-n_\rho) &= \left[ \frac{1}{2\pi} \int_{-\pi}^{+\pi} \mathbf{J}_E(n_\rho, \tau, n_{z\pm}(n_\rho)) e^{-jm(\tau+\pi)} d\tau \right. \\
&\quad \left. + \operatorname{sgn}(z) \frac{1}{2\pi} \int_{-\pi}^{+\pi} \mathbf{J}_O(n_\rho, \tau, n_{z\pm}(n_\rho)) e^{-jm(\tau+\pi)} d\tau \right] \\
&= (-1)^m [\mathbf{d}_{m\pm}^E(n_\rho) + \operatorname{sgn}(z) \mathbf{d}_{m\pm}^O(n_\rho)] \tag{B6}
\end{aligned}$$

Using equation (B4) the proof of the relation (23) in section 3 is closed.

## Appendix C: Coefficients of the Polynomial Equation

[45] The equation to find the saddle points can be transformed to a sextic equation

$$\begin{aligned}
a_6 \tau^6 + a_5 \tau^5 + a_4 \tau^4 + a_3 \tau^3 + a_2 \tau^2 + a_1 \tau + a_0 &= 0 \\
\tau &= n_\rho^2
\end{aligned} \tag{C1}$$

The coefficients in the equation are

$$\begin{aligned}
a_6 &= \varepsilon_1(\varepsilon_1 - \varepsilon_3)^4(\varepsilon_1 \cos^2 \alpha + \varepsilon_3 \sin^2 \alpha) \\
a_5 &= -(\varepsilon_1 - \varepsilon_3)^2 \left\{ \begin{aligned} &8\varepsilon_1^2 \varepsilon_2^2 \varepsilon_3 \cos^4 \alpha \\ &+ \left[ -\varepsilon_2^2(\varepsilon_1 + \varepsilon_3)(\varepsilon_1^2 + \varepsilon_3^2 - 10\varepsilon_1 \varepsilon_3) \right. \\ &\quad \left. + \varepsilon_1(\varepsilon_1 - \varepsilon_3)^2(\varepsilon_1^2 + \varepsilon_3^2) \right] \sin^2 \alpha \cos^2 \alpha \\ &+ \varepsilon_3 \left[ -\varepsilon_2^2(\varepsilon_1^2 + \varepsilon_3^2 - 10\varepsilon_1 \varepsilon_3) \right. \\ &\quad \left. + \varepsilon_1(\varepsilon_1 + \varepsilon_3)(\varepsilon_1 - \varepsilon_3)^2 \right] \sin^4 \alpha \end{aligned} \right\} \\
a_4 &= \left\{ \begin{aligned} &2\varepsilon_2^2 \left[ \varepsilon_1 \varepsilon_3 (\varepsilon_1^2 - \varepsilon_3^2)^2 - \varepsilon_2^2 \varepsilon_1 \varepsilon_3 (\varepsilon_1^2 + \varepsilon_3^2 - 10\varepsilon_1 \varepsilon_3) \right] \cos^4 \alpha \\ &+ \varepsilon_2^2 \varepsilon_3 \left[ (\varepsilon_1 - \varepsilon_3)^2 (7\varepsilon_1^3 + 17\varepsilon_1 \varepsilon_3^2 + 9\varepsilon_2^2 \varepsilon_3 - \varepsilon_3^3) \right. \\ &\quad \left. - \varepsilon_2^2 (\varepsilon_1 + \varepsilon_3) (7\varepsilon_1^2 + 7\varepsilon_3^2 - 30\varepsilon_1 \varepsilon_3) \right] \sin^2 \alpha \cos^2 \alpha \\ &+ \varepsilon_3^2 \left[ \varepsilon_1^2 (\varepsilon_1 - \varepsilon_3)^4 + \varepsilon_2^2 (\varepsilon_1 - \varepsilon_3)^2 (7\varepsilon_1^2 + 18\varepsilon_1 \varepsilon_3 - \varepsilon_3^2) \right. \\ &\quad \left. - 8\varepsilon_2^4 (\varepsilon_1^2 + \varepsilon_3^2 - 4\varepsilon_1 \varepsilon_3) \right] \sin^4 \alpha \end{aligned} \right\} \\
a_3 &= 2\varepsilon_2^2 \varepsilon_3 \left\{ \begin{aligned} &[-4\varepsilon_1 \varepsilon_3 \varepsilon_2^2 (\varepsilon_1 + \varepsilon_3)^2 + 4\varepsilon_2^4 \varepsilon_1 \varepsilon_3] \cos^4 \alpha \\ &+ \left[ -\varepsilon_1 \varepsilon_3 (\varepsilon_1 - \varepsilon_3)^2 (3\varepsilon_1^2 + 3\varepsilon_3^2 + 2\varepsilon_1 \varepsilon_3) \right. \\ &\quad \left. - \varepsilon_2^2 \varepsilon_3 (3\varepsilon_1^3 + 20\varepsilon_1^2 \varepsilon_3 + 31\varepsilon_1 \varepsilon_3^2 - 6\varepsilon_3^3) \right. \\ &\quad \left. + 6\varepsilon_2^4 \varepsilon_3 (\varepsilon_1 + \varepsilon_3) \right] \sin^2 \alpha \cos^2 \alpha \\ &+ 4\varepsilon_3^2 \left[ -\varepsilon_1 (\varepsilon_1 - \varepsilon_3)^2 (2\varepsilon_1 + \varepsilon_3) \right. \\ &\quad \left. + 2\varepsilon_2^2 \varepsilon_3 (\varepsilon_3 - 5\varepsilon_1) + 2\varepsilon_2^4 \right] \sin^4 \alpha \end{aligned} \right\} \\
a_2 &= \varepsilon_2^2 \varepsilon_3^2 \left\{ \begin{aligned} &\varepsilon_2^2 [(\varepsilon_1 + \varepsilon_3)^4 + \varepsilon_2^4 - 2\varepsilon_2^2 (\varepsilon_1 + \varepsilon_3)^2] \cos^4 \alpha \\ &+ 4\varepsilon_2^2 \varepsilon_3 \left[ (5\varepsilon_1^3 + 9\varepsilon_1^2 \varepsilon_3 + 11\varepsilon_1 \varepsilon_3^2 - \varepsilon_3^3) \right. \\ &\quad \left. - \varepsilon_2^2 (5\varepsilon_1 + 7\varepsilon_3) \right] \sin^2 \alpha \cos^2 \alpha \\ &+ 8\varepsilon_3^2 \left[ \varepsilon_1^2 (\varepsilon_1 - \varepsilon_3)^2 + \varepsilon_2^2 (5\varepsilon_1^2 + 8\varepsilon_1 \varepsilon_3 - \varepsilon_3^2) - 6\varepsilon_2^4 \right] \sin^4 \alpha \end{aligned} \right\} \\
a_1 &= 8\varepsilon_2^4 \varepsilon_3^4 \left\{ \begin{aligned} &[\varepsilon_2^2 (\varepsilon_1 + 2\varepsilon_3) - \varepsilon_1 (\varepsilon_1 + \varepsilon_3)^2] \cos^2 \alpha \\ &+ 2\varepsilon_3 [3\varepsilon_2^2 - 3\varepsilon_1^2 - \varepsilon_1 \varepsilon_3] \sin^2 \alpha \end{aligned} \right\} \sin^2 \alpha \\
a_0 &= 16\varepsilon_2^4 \varepsilon_3^6 (\varepsilon_1 - \varepsilon_2^2) \sin^4 \alpha \quad (C2)
\end{aligned}$$

The components of the far field in the Cartesian coordinate system are derived from equation (12) as

$$\begin{aligned}
E_{x\pm}(\mathbf{r}) &= k_0^4 \left\{ \begin{aligned} &(n_{ps}^2 Q_{\pm} \cos^2 \beta - R_{\pm}) A_{x\pm}(\mathbf{r}) \\ &+ (n_{ps}^2 Q_{\pm} \sin \beta \cos \beta - j\varepsilon_2 U) A_{y\pm}(\mathbf{r}) \\ &+ n_{ps} \|n_{z\pm}\| (P_{\pm} \cos \beta - j\varepsilon_2 \sin \beta) A_{z\pm}(\mathbf{r}) \end{aligned} \right\} \\
E_{y\pm}(\mathbf{r}) &= k_0^4 \left\{ \begin{aligned} &(n_{ps}^2 Q_{\pm} \sin \beta \cos \beta + j\varepsilon_2 U) A_{x\pm}(\mathbf{r}) \\ &+ (n_{ps}^2 Q_{\pm} \sin^2 \beta - R_{\pm}) A_{y\pm}(\mathbf{r}) \\ &+ n_{ps} \|n_{z\pm}\| (P_{\pm} \sin \beta + j\varepsilon_2 \cos \beta) A_{z\pm}(\mathbf{r}) \end{aligned} \right\} \\
E_{z\pm}(\mathbf{r}) &= k_0^4 \left\{ \begin{aligned} &n_{ps} \|n_{z\pm}\| (P_{\pm} \cos \beta + j\varepsilon_2 \sin \beta) A_{x\pm}(\mathbf{r}) \\ &+ n_{ps} \|n_{z\pm}\| (P_{\pm} \sin \beta - j\varepsilon_2 \cos \beta) A_{y\pm}(\mathbf{r}) \\ &+ [n_{ps}^2 V_{\pm} + n_{z\pm}^2 (V_{\pm} - \varepsilon_1) + (\varepsilon_1^2 - \varepsilon_2^2)] A_{z\pm}(\mathbf{r}) \end{aligned} \right\} \\
H_{x\pm}(\mathbf{r}) &= \frac{k_0^5}{\mu_0 \omega} \left\{ \begin{aligned} &\|n_{z\pm}\| \left[ \begin{aligned} &-(\varepsilon_1 - \varepsilon_3) n_{ps}^2 \sin \beta \cos \beta \\ &-j\varepsilon_2 n_{ps}^2 \cos^2 \beta + j\varepsilon_2 \varepsilon_3 \end{aligned} \right] A_{x\pm}(\mathbf{r}) \\ &+ \|n_{z\pm}\| \left[ \begin{aligned} &\varepsilon_1 n_{ps}^2 \cos^2 \beta + \varepsilon_3 n_{ps}^2 \sin^2 \beta \\ &-j\varepsilon_2 n_{ps}^2 \sin \beta \cos \beta + \varepsilon_3 n_{z\pm}^2 - \varepsilon_1 \varepsilon_3 \end{aligned} \right] A_{y\pm}(\mathbf{r}) \\ &+ n_{ps} \left[ \begin{aligned} &-(\varepsilon_1 (n_{ps}^2 + n_{z\pm}^2) - (\varepsilon_1^2 - \varepsilon_2^2)) \sin \beta \\ &-j\varepsilon_2 n_{z\pm}^2 \cos \beta \end{aligned} \right] A_{z\pm}(\mathbf{r}) \end{aligned} \right\} \\
H_{y\pm}(\mathbf{r}) &= \frac{k_0^5}{\mu_0 \omega} \left\{ \begin{aligned} &\|n_{z\pm}\| \left[ \begin{aligned} &-\varepsilon_1 n_{ps}^2 \sin^2 \beta - \varepsilon_3 n_{ps}^2 \cos^2 \beta \\ &-j\varepsilon_2 n_{ps}^2 \sin \beta \cos \beta - \varepsilon_3 n_{z\pm}^2 + \varepsilon_1 \varepsilon_3 \end{aligned} \right] A_{x\pm}(\mathbf{r}) \\ &+ \|n_{z\pm}\| \left[ \begin{aligned} &(\varepsilon_1 - \varepsilon_3) n_{ps}^2 \sin \beta \cos \beta \\ &-j\varepsilon_2 n_{ps}^2 \sin^2 \beta + j\varepsilon_2 \varepsilon_3 \end{aligned} \right] A_{y\pm}(\mathbf{r}) \\ &+ n_{ps} \left[ \begin{aligned} &(\varepsilon_1 (n_{ps}^2 + n_{z\pm}^2) - (\varepsilon_1^2 - \varepsilon_2^2)) \cos \beta \\ &-j\varepsilon_2 n_{z\pm}^2 \sin \beta \end{aligned} \right] A_{z\pm}(\mathbf{r}) \end{aligned} \right\} \\
H_{z\pm}(\mathbf{r}) &= \frac{k_0^5}{\mu_0 \omega} \left\{ \begin{aligned} &n_{ps} (R_{\pm} \sin \beta + j\varepsilon_2 U \cos \beta) A_{x\pm}(\mathbf{r}) \\ &-n_{ps} (R_{\pm} \cos \beta - j\varepsilon_2 U \sin \beta) A_{y\pm}(\mathbf{r}) \\ &+ j\varepsilon_2 n_{ps}^2 \|n_{z\pm}\| A_{z\pm}(\mathbf{r}) \end{aligned} \right\} \quad (D3)
\end{aligned}$$

## Appendix D: Far Field Components

[46] Using the computation rule given by equation (50) in section 6, the elements of the differential operator as given by (A1) for either mode can all be reduced to factors,

$$\begin{aligned}
\Lambda_{11} &= k_0^4 (n_{ps}^2 Q_{\pm} \cos^2 \beta - R_{\pm}) \\
\Lambda_{12} &= k_0^4 (n_{ps}^2 Q_{\pm} \sin \beta \cos \beta - j\varepsilon_2 U) \\
\Lambda_{13} &= k_0^4 n_{ps} \|n_{z\pm}\| (P_{\pm} \cos \beta - j\varepsilon_2 \sin \beta) \\
\Lambda_{21} &= k_0^4 (n_{ps}^2 Q_{\pm} \sin \beta \cos \beta + j\varepsilon_2 U) \\
\Lambda_{22} &= k_0^4 (n_{ps}^2 Q_{\pm} \sin^2 \beta - R_{\pm}) \\
\Lambda_{23} &= k_0^4 n_{ps} \|n_{z\pm}\| (P_{\pm} \sin \beta + j\varepsilon_2 \cos \beta) \\
\Lambda_{31} &= k_0^4 n_{ps} \|n_{z\pm}\| (P_{\pm} \cos \beta + j\varepsilon_2 \sin \beta) \\
\Lambda_{32} &= k_0^4 n_{ps} \|n_{z\pm}\| (P_{\pm} \sin \beta - j\varepsilon_2 \cos \beta) \\
\Lambda_{33} &= k_0^4 [n_{ps}^2 V_{\pm} + n_{z\pm}^2 (V_{\pm} - \varepsilon_1) + (\varepsilon_1^2 - \varepsilon_2^2)]
\end{aligned} \quad (D1)$$

where

$$\begin{aligned}
P_{\pm} &= n_{ps}^2 + n_{z\pm}^2 - \varepsilon_1 \\
Q_{\pm} &= n_{ps}^2 + n_{z\pm}^2 - \varepsilon_3 \\
R_{\pm} &= \varepsilon_1 n_{ps}^2 + \varepsilon_3 n_{z\pm}^2 - \varepsilon_1 \varepsilon_3 \\
U &= n_{ps}^2 - \varepsilon_3 \\
V_{\pm} &= n_{z\pm}^2 - \varepsilon_1 \\
\|n_{z\pm}\| &= n_{z\pm} \operatorname{sgn}(\pi/2 - \alpha)
\end{aligned} \quad (D2)$$

Transforming to the spherical coordinate system and replacing the subscripts  $(x, y, z)$  with  $(1, 2, 3)$ , the components of the far field take the form

$$\begin{aligned}
E_{r\pm}(\mathbf{r}) &= \frac{\mu_0 \omega}{2\pi} F_{1\pm}(\alpha) \left[ \sum_{i=1}^3 J_{i\pm}(n_{ps}, \beta, \|n_{z\pm}\|) F_{Eri\pm} \right] \frac{e^{-jk_0 n_s r}}{r} \\
E_{\alpha\pm}(\mathbf{r}) &= \frac{\mu_0 \omega}{2\pi} F_{1\pm}(\alpha) \left[ \sum_{i=1}^3 J_{i\pm}(n_{ps}, \beta, \|n_{z\pm}\|) F_{E\alpha i\pm} \right] \frac{e^{-jk_0 n_s r}}{r} \\
E_{\beta\pm}(\mathbf{r}) &= \frac{\mu_0 \omega}{2\pi} F_{1\pm}(\alpha) \left[ \sum_{i=1}^3 J_{i\pm}(n_{ps}, \beta, \|n_{z\pm}\|) F_{E\beta i\pm} \right] \frac{e^{-jk_0 n_s r}}{r} \\
H_{r\pm}(\mathbf{r}) &= \frac{k_0}{2\pi} F_{1\pm}(\alpha) \left[ \sum_{i=1}^3 J_{i\pm}(n_{ps}, \beta, \|n_{z\pm}\|) F_{Hri\pm} \right] \frac{e^{-jk_0 n_s r}}{r} \\
H_{\alpha\pm}(\mathbf{r}) &= \frac{k_0}{2\pi} F_{1\pm}(\alpha) \left[ \sum_{i=1}^3 J_{i\pm}(n_{ps}, \beta, \|n_{z\pm}\|) F_{H\alpha i\pm} \right] \frac{e^{-jk_0 n_s r}}{r} \\
H_{\beta\pm}(\mathbf{r}) &= \frac{k_0}{2\pi} F_{1\pm}(\alpha) \left[ \sum_{i=1}^3 J_{i\pm}(n_{ps}, \beta, \|n_{z\pm}\|) F_{H\beta i\pm} \right] \frac{e^{-jk_0 n_s r}}{r}
\end{aligned} \quad (D4)$$

where the factors,  $F_{Er1\pm}$ ,  $F_{Er2\pm}$ ,  $F_{Er3\pm}$ ,  $F_{E\alpha1\pm}$ ,  $F_{E\alpha2\pm}$ ,  $F_{E\alpha3\pm}$ ,  $F_{E\beta1\pm}$ ,  $F_{E\beta2\pm}$ ,  $F_{E\beta3\pm}$ ,  $F_{Hr1\pm}$ ,  $F_{H\alpha1\pm}$ ,  $F_{H\beta1\pm}$ ,  $F_{H\beta2\pm}$ ,  $F_{H\beta3\pm}$  etc. read as

$$\begin{aligned}
 F_{Er1\pm} &= \left\{ \begin{aligned} &UP_{\pm} \sin \alpha \cos \beta + j\epsilon_2 U \sin \alpha \sin \beta \\ &+ n_{ps} \|n_{z\pm}\| P_{\pm} \cos \alpha \cos \beta + j\epsilon_2 n_{ps} \|n_{z\pm}\| \cos \alpha \sin \beta \end{aligned} \right\} \\
 F_{Er2\pm} &= \left\{ \begin{aligned} &UP_{\pm} \sin \alpha \sin \beta - j\epsilon_2 U \sin \alpha \cos \beta \\ &+ n_{ps} \|n_{z\pm}\| P_{\pm} \cos \alpha \sin \beta - j\epsilon_2 n_{ps} \|n_{z\pm}\| \cos \alpha \cos \beta \end{aligned} \right\} \\
 F_{Er3\pm} &= \{n_{ps} \|n_{z\pm}\| P_{\pm} \sin \alpha + (V_{\pm} P_{\pm} - \epsilon_2^2) \cos \alpha\} \\
 F_{E\alpha1\pm} &= \left\{ \begin{aligned} &UP_{\pm} \cos \alpha \cos \beta + j\epsilon_2 U \cos \alpha \sin \beta \\ &- n_{ps} \|n_{z\pm}\| P_{\pm} \sin \alpha \cos \beta - j\epsilon_2 n_{ps} \|n_{z\pm}\| \sin \alpha \sin \beta \end{aligned} \right\} \\
 F_{E\alpha2\pm} &= \left\{ \begin{aligned} &UP_{\pm} \cos \alpha \sin \beta - j\epsilon_2 U \cos \alpha \cos \beta \\ &- n_{ps} \|n_{z\pm}\| P_{\pm} \sin \alpha \sin \beta + j\epsilon_2 n_{ps} \|n_{z\pm}\| \sin \alpha \cos \beta \end{aligned} \right\} \\
 F_{E\alpha3\pm} &= \{n_{ps} \|n_{z\pm}\| P_{\pm} \cos \alpha - (V_{\pm} P_{\pm} - \epsilon_2^2) \sin \alpha\} \\
 F_{E\beta1\pm} &= \{R_{\pm} \sin \beta + j\epsilon_2 U \cos \beta\} \\
 F_{E\beta2\pm} &= \{-R_{\pm} \cos \beta + j\epsilon_2 U \sin \beta\} \\
 F_{E\beta3\pm} &= \{j\epsilon_2 n_{ps} \|n_{z\pm}\|\} \\
 F_{Hr1\pm} &= \{F_{E\beta i\pm} (n_{ps} \cos \alpha - \|n_{z\pm}\| \sin \alpha)\}, i = 1, 2, 3 \\
 F_{H\alpha i\pm} &= \{-F_{E\beta i\pm} (n_{ps} \sin \alpha + \|n_{z\pm}\| \cos \alpha)\}, i = 1, 2, 3 \\
 F_{H\beta1\pm} &= \{-\epsilon_3 \|n_{z\pm}\| P_{\pm} \cos \beta - j\epsilon_2 \epsilon_3 \|n_{z\pm}\| \sin \beta\} \\
 F_{H\beta2\pm} &= \{-\epsilon_3 \|n_{z\pm}\| P_{\pm} \sin \beta + j\epsilon_2 \epsilon_3 \|n_{z\pm}\| \cos \beta\} \\
 F_{H\beta3\pm} &= \{n_{ps} [\epsilon_1 P_{\pm} + \epsilon_2^2]\} \tag{D5}
 \end{aligned}$$

[47] **Acknowledgments.** Xueqin Huang has, in part, been supported by Air Force contracts FA8718-06-C-0072 and FA8718-05-C-0027 and by a grant from Lowell Digisonde International, LLC.

## References

- Arbel, E., and L. B. Felsen (1963), Theory of radiation from sources in anisotropic media. Part II: Point source in infinite, homogeneous medium, in *Electromagnetic Theory and Antennas: Proceedings of a Symposium*, edited by E. C. Jordan, pp. 421–459, Pergamon, New York.
- Balmain, K. (1964), The impedance of a short dipole antenna in a magneto-plasma, *IEEE Trans. Antennas Propag.*, *12*, 605–617, doi:10.1109/TAP.1964.1138278.
- Bayin, Ş. S. (2006a), Integral equations, in *Mathematical Methods in Science and Engineering*, chap. 18, pp. 547–566, Wiley-Interscience, Hoboken, N. J., doi:10.1002/0470047429.
- Bayin, Ş. S. (2006b), Green's functions, in *Mathematical Methods in Science and Engineering*, chap. 19, pp. 567–632, Wiley-Interscience, Hoboken, N. J., doi:10.1002/0470047429.
- Bennett, J. A. (1976), The Green's function for waves in a homogeneous anisotropic absorbing plasma, *J. Plasma Phys.*, *15*, 133–150, doi:10.1017/S002237780001967X.
- Budden, K. G. (1985), *The Propagation of Radio Waves: The Theory of Radio Waves of Low Power in the Ionosphere and Magnetosphere*, Cambridge Univ. Press, Cambridge, U. K., doi:10.1017/CBO9780511564321.
- Chevalier, T. W., U. S. Inan, and T. F. Bell (2008), Terminal impedance and antenna current distribution of a VLF electric dipole in the inner magnetosphere, *IEEE Trans. Antennas Propag.*, *56*, 2454–2468.
- Cottis, P. G., C. N. Vazouras, and C. Spyrou (1999), Green's function for an unbounded biaxial medium in cylindrical coordinates, *IEEE Trans. Antennas Propag.*, *47*, 195–199, doi:10.1109/8.753010.
- Felsen, L. B., and N. Marcuvitz (1994), *Radiation and Scattering of Waves*, IEEE Press, Piscataway, N. J.
- Fung, P. C. W., and T. P. Kwan (1983), Theory of radiation in an anisotropic plasma, *Astrophys. Space Sci.*, *93*(2), 281–293, doi:10.1007/BF00648737.
- Fung, S. F., and J. L. Green (2005), Modeling of field-aligned guided echoes in the plasmasphere, *J. Geophys. Res.*, *110*, A01210, doi:10.1029/2004JA010658.
- Kaklamani, D. I., and N. K. Uzunoglu (1992), Radiation of a dipole in an infinite triaxial anisotropic medium, *Electromagnetics*, *12*, 231–245, doi:10.1080/02726349208908313.
- Kogelnik, H. (1960), On electromagnetic radiation in magneto-ionic media, *J. Res. Natl. Bur. Stand. U.S., Sect. D*, *64D*, 515–523.
- Lai, H. M., and P. K. Chan (1986), Far field and energy flux caused by a radiating source in an anisotropic medium, *Phys. Fluids*, *29*(6), 1881–1890, doi:10.1063/1.865617.
- Novikov, V. V., and S. T. Rybachek (1990), Electromagnetic fields of elementary radiators in a homogeneous anisotropic plasma [in Russian], *Geomagn. Aeron.*, *30*, 227–235.
- Rasmussen, C. E., P. M. Banks, and K. J. Harker (1986), The minimum distance to the far field in a magnetized plasma, *Radio Sci.*, *21*(6), 920–928, doi:10.1029/RS021i006p00920.
- Reinisch, B. W., et al. (2000), The Radio Plasma Imager investigation on the IMAGE spacecraft, *Space Sci. Rev.*, *91*, 319–359, doi:10.1023/A:1005252602159.
- Reinisch, B. W., X. Huang, P. Song, G. S. Sales, S. F. Fung, J. L. Green, D. L. Gallagher, and V. M. Vasyliunas (2001), Plasma density distribution along the magnetospheric field: RPI observations from IMAGE, *Geophys. Res. Lett.*, *28*, 4521–4524, doi:10.1029/2001GL013684.
- Rybachek, S. T. (1995), Radio wave propagation from antennae at satellite altitudes into the Earth-ionosphere waveguide, *J. Atmos. Terr. Phys.*, *57*(3), 303–309, doi:10.1016/0021-9169(94)E0002-5.
- Rybachek, S. T., V. I. Ivanov, and V. L. Senina (1997), Ionospheric fields excited by sources located in the Earth-ionosphere irregular waveguide, *J. Atmos. Sol. Terr. Phys.*, *59*(1), 139–149, doi:10.1016/1364-6826(95)00195-6.
- Seshadri, S. R., and T. T. Wu (1970), Radiation condition for a magneto-plasma medium, *Q. J. Mech. Appl. Math.*, *23*, 285–313, doi:10.1093/qjmam/23.2.285.
- Stix, T. H. (1992), *Waves in Plasmas*, Am. Inst. Phys., New York.
- Stratton, J. A. (1941), *Electromagnetic Theory*, McGraw-Hill, New York.
- Swanson, D. G. (1989), *Plasma Waves*, Academic, Boston, Mass.
- Weiglhofer, W. S. (1993), Analytic methods and free-space dyadic Green's functions, *Radio Sci.*, *28*(5), 847–857, doi:10.1029/93RS00903.

X. Huang, Center for Atmospheric Research, University of Massachusetts Lowell, 600 Suffolk St., Lowell, MA 01854, USA. (xueqin\_huang@uml.edu)  
 B. W. Reinisch, Lowell Digisonde International, LLC, 175 Cabot St., Lowell, MA 01854, USA. (bodo.reinisch@digisonde.com)